UNIVERSIDADE FEDERAL DO CEARÁ
CENTRO DE CIÊNCIAS
DEPARTAMENTO DE QUÍMICA ANALÍTICA E FÍSICO-QUÍMICA
PROGRAMA DE PÓS-GRADUAÇÃO EM QUÍMICA

LUCAS PINHEIRO COUTINHO

USE OF COMPUTATIONAL METHODS IN THE STUDY OF CHEMICAL REACTIONS OF PSYCHEDELICS AND INTERSTELLAR MOLECULES: *N*,*N*-DIMETHYLTRYPTAMINE AND PROPARGYLIMINE

FORTALEZA
2023

LUCAS PINHEIRO COUTINHO

USE OF COMPUTATIONAL METHODS IN THE STUDY OF CHEMICAL REACTIONS OF PSYCHEDELICS AND INTERSTELLAR MOLECULES: *N*,*N*-DIMETHYLTRYPTAMINE AND PROPARGYLIMINE

Dissertação apresentada ao Programa de Pós-Graduação em Química da Universidade Federal do Ceará, como requisito parcial à obtenção do título de Mestre em Química. Área de concentração: Físico-química.

Orientador: Prof. Dr. Norberto de Kássio Vieira Monteiro.
Coorientador: Dr. Sérgio Ruschi Bergamachi Silva.

FORTALEZA

2023

Dados Internacionais de Catalogação na Publicação
Universidade Federal do Ceará
Sistema de Bibliotecas
Gerada automaticamente pelo módulo Catalog, mediante os dados fornecidos pelo(a) autor(a)

C896u Coutinho, Lucas Pinheiro.
Use of computational methods in the study of chemical reactions of psychedelics and interstellar molecules : N,N-dimethyltryptamine and propargylimine / Lucas Pinheiro Coutinho. – 2023.
78 f. : il. color.

Dissertação (mestrado) – Universidade Federal do Ceará, Centro de Ciências, Programa de Pós-Graduação em Química, Fortaleza, 2023.
Orientação: Prof. Dr. Norberto de Kássio Vieira Monteiro.
Coorientação: Prof. Dr. Sérgio Ruschi Bergamachi.

1. N,N-dimethyltryptamine. 2. Propargylimine. 3. Mechanism. 4. Density functional theory. 5. Potential energy surface . I. Título.

CDD 540

LUCAS PINHEIRO COUINHO

USE OF COMPUTATIONAL METHODS IN THE STUDY OF CHEMICAL REACTIONS OF PSYCHEDELICS AND INTERSTELLAR MOLECULES: *N*,*N*-DIMETHYLTRYPTAMINE AND PROPARGYLIMINE

Dissertação apresentada ao Programa de Pós-Graduação em Química da Universidade Federal do Ceará, como requisito parcial à obtenção do título de Mestre em Química. Área de concentração: Físico-química.

Aprovada em: xx/xx/xxxx.

BANCA EXAMINADORA

_____

Prof. Dr. Norberto de Kássio Vieira Monteiro (Orientador)
Universidade Federal do Ceará (UFC)

_____

Dr. Sérgio Ruschi Bergamachi (Coorientador)
Universidade Federal do Rio Grande do Norte (UFRN)

_____

Prof. Dr. Paulo Naftali da Silva Casciano
Instituto Federal do Ceará (UFC)

_____

Prof. Dr. Pedro de Lima-Neto
Universidade Federal do Ceará (UFC)

In memory of Baruch Spinoza, who revealed the true substance of the Cosmos; of Immanuel Kant, which helped humanity to reach its maturity; of Carl Sagan, whose passion for science always touched my heart and of Socrates, whose foundation of reasoning itself he demonstrated through being humble.

ACKNOWLEDGMENTS

Firstly, I would like to thank my parents, Emanuel Ferreira Coutinho and Ana Paula Pinheiro de Matos, which existence is of utmost importance to me, since I would not be here without them. To my father I express gratitude for the simple ideal he represents, my model to all life. To mother I thank the love, sometimes difficult, but always sincere.

To my stepmother, Carla Ilane Moreira Bezerra, I thank the presence which was paramount to my stability in youth days.

To my siblings, Maria Paula Pinheiro de Souza and Miguel Moreira Coutinho. To my sister I thank all the good moments of our youth, may you become whatever you wish to be. To my little brother I thank the reminder of how good it is to be a child.

My lovely gratitude to my inspiration and my eternal companion, Nicaely Maria de Oliveira Pereira, this work would never been done without your advice, help and most important, your love, since the basis of all human existence is this, love, and only this.

To all my friends and colleagues in the Grupo de Química Teórica (GQT): Renato Veríssimo de Oliveira, José Osmar de Souza Júnior, Lucas Lima Bezerra and Leonardo Paes da Silva, whose friendship has helped me in difficult times and intelligence helped me in the ways of chemistry. To Leo, I thank the heroic discussions and whose plenitude was always inspiring, To Lucas, I thank the muscular discussions and the demonstration that is possible to overcome great odds with mental strength. To Osmar, I thank the philosophical discussions and also your serenity state in which you influenced in me. Finally to Renato, whose UFC gave not only a friend but also a brother. May you accomplish all your goals, but above all cultivate happiness in this precious, but finite life.

My gratitude to dear professors: Prof. Dr. Norberto de Kássio Vieira Monteiro, Dr. Sérgio Ruschi Bergamachi, Prof. Dr. José Roberval Cândido Júnior and Prof. Dr. Pedro de Lima-Neto. My special thanks to my professor Norberto Monteiro, which accepted me since undergraduation. The day I first enter GQT was the beginning of my true journey through science. All this happened because of the doors professor Norberto opened to me.

My gratitude to the Universidade Federal do Ceará (UFC) and the Programa de Pós-gradução em Química (PGQUIM) for the opportunity to participate in such prestigious institutions, and the for the financial support of the Conselho Nacional de Desenvolvimento Científico e Tecnologico (CNPq) (process number: 160588/2021-9 and validity from 01/10/2021 to 30/09/2023), which provide my master’s degree scholarship.

My final gratitude to all thinkers and artists who develop all the knowledge needed to do my present work.

“Two things awe me the most, the starry sky above me and the moral law within me.” Immanuel Kant.

RESUMO

Métodos computacionais podem ser usados para estudar sistemas químicos a fim de fornecer uma miríade de *insights* sobre mecanismos de reação. De métodos baseados em densidade eletrônica a métodos de mecânica molecular, a química teórica está no estado da arte da química atual. Portanto, o presente estudo reúne dois artigos que exemplificam a química computacional como uma ferramenta para a química moderna: *insights* mecanísticos da biossíntese do psicodélico *N*,*N*-dimetiltriptamina (DMT) e da propargilimina (PGIM) presente no meio interestelar (ISM). No Capítulo I, a DMT, um produto psicoativo endogenamente humano, faz parte da rota do L-triptofano, dividida na descarboxilação por uma L-aminoácido descarboxilase aromática (AADC) para formação de triptamina (etapa elucidada) e a subsequente dupla-metilação pela indoletilamina-*N*-metiltransferase (INMT) através do cofator *S*-adenosil-L-metionina (SAM) (etapa não elucidada). Portanto, um modelo *in silico*, usando cálculos ONIOM QM:MM, foi proposto com base no perfil S_N2 da superfície de energia potencial (PES) construída, mostrando a segunda barreira de energia de metilação sendo a etapa limitante com $\delta G^{\ddagger} = 14.65\ \text{kcal} \cdot \text{mol}^{-1}$ maior que a metilação anterior. Além disso, os estados de hibridização de cada etapa da reação foram examinados para acompanhar a mudança de geometria ao longo da coordenada da reação. No Capítulo II, a imina PGIM, uma molécula orgânica complexa (iCOM) no ISM, é investigada, seguindo um modelo semelhante a síntese Strecker, com um mecanismo de duas etapas: condensação de propinal e amônia e uma subsequente eliminação de uma molécula de água formando o PGIM. A construção do PES foi realizada com o nível teórico wB97XD/aug-ccp-VTZ, em meio de fase gasosa nas temperaturas de 10 e 298 K, mostrando que a segunda barreira de energia é a etapa limitante em ambas as temperaturas. Além disso, cálculos de teoria quântica de átomos em moléculas (QTAIM) foram feitos para analisar a densidade eletrônica obtida e os estados de hibridização dos estados de transição foram usados para entender a geometria das barreiras de energia.

Keywords: *N*,*N*-Dimetiltriptamina (DMT); propargilimina (PGIM); mecanismo; ONIOM; teoria do funcional da densidade (DFT); superfície de energia potencial (PES); psicoativos; meio interestelar.

ABSTRACT

Computational methods can be used to study chemical systems in order to give a myriad of insights about reaction mechanisms. From electron density based methods to molecular mechanic ones. Nonetheless, theoretical chemistry is at the state-of-the-art of current chemistry endeavour. Therefore, the present study, brings together two essays which exemplifies computational chemistry as a tool to modern chemistry: mechanistic insights of the biosynthesis of the psychedelic *N*,*N*-dimethyltryptamine (DMT) and the interstellar medium (ISM) molecule propargylimine (PGIM). In Chapter I, DMT, an endogenously human psychoactive product, is part of the L-tryptophan pathway, divided into the decarboxylation by an aromatic L-amino acid decarboxylase (AADC) for tryptamine formation (elucidated step) and the subsequent double-methylation by the indolethylamine-*N*-methyltransferase (INMT) through the cofactor *S*-adenosyl-L-methionine (SAM) (not elucidated step). Therefore, an *in silico* model, using ONIOM QM:MM calculations, was proposed based on the build S_N2 potential energy surface (PES) profile, showing the second methylation energy barrier being the rate-limiting step with $\delta G^{\ddagger} = 14.65\ \text{kcal} \cdot \text{mol}^{-1}$ larger than the previous methylation. Besides, hybridization states of each reaction step were examined to follow geometry change along the reaction coordinate. In Chapter II, PGIM, an imine interstellar complex organic molecule (iCOM), is investigated, following a Strecker-type synthesis model, with a two-step mechanism: condensation of propynal and ammonia and a subsequent elimination of water molecule forming PGIM. The built PES was performed with wB97XD/aug-ccp-VTZ level of theory, in gas phase medium at temperatures of 10 and 298 K, showing the second energy barrier to be the rate-limiting step in both temperatures. Additionally, Quantum theory of atoms in molecules (QTAIM) calculations were done to analyse the obtained electron density and the hybridization states of the transition states were used to understand the geometrical of the energy barriers.

Keywords: *N*,*N*-Dimethyltryptamine (DMT); propargylimine (PGIM); mechanism; ONIOM; density functional theory (DFT); potential energy surface (PES); psychoactives; interstellar medium.

LIST OF ABBREVIATIONS AND ACRONYMS

5-HT	Serotonin
5-HTP	5-hydroxytryptophan
AADC	Aromatic L-amino acid decarboxylase
B3LYP	Becke's three-parameter functional with the Lee-Yang-Parr correlation functional
D3	Grimme D3 dispersion corrections
DFT	Density functional theory
DMT	*N*,*N*-dimethyltryptamine
DNA	Deoxyribonucleic acid
E2	Bimolecular elimination
ELF	Electron localization function
iCOM	Interstellar complex organic molecule
Ind	Indol
INMT	Indolethylamine-*N*-methyltransferase
IRC	Intrinsic reaction coordinates
ISM	Interstellar medium
LSD	Lysergic acid diethylamide
MD	Molecular dynamics
ME	Mechanical embedding
MT	*N*-methyltryptamine
NCI	Non-covalent interactions
NPT	Isothermic-isobaric ensemble
NVT	Canonical ensemble
ONIOM	Our own n-layered Integrated Molecular Orbital and Molecular Mechanics
PDB	Protein Data Bank
PES	Potential energy surface
PGIM	Propargylimine
PLP	Pyridoxalphosphate
PME	Particle mesh Ewald
QM:MM	Quantum Mechanics and Molecular Mechanics
QTAIM	Quantum theory of atoms in molecules
RNA	Ribonucleic acid

SAH	*S*-adenosyl-L-homocysteine
SAM	*S*-adenosyl-L-methionine
S_N2	Bimolecular Nucleophilic Substitution
TIP3P	Transferable intermolecular potential with 3 point
Tryp	Typtamine
UFF	Universal Force Field

SUMMARY

1 INTRODUCTION

1.1 *N*,*N*-Dimethyltryptamine psychedelia

Psychoactive plants are part of our daily lives, from *Coffea arabica* beans used in our morning breakfast coffees to the diverse use of herbal leaves to prepare delightful teas at afternoon meals (ADAN, 1994). Employed by millennia, the consumption of psychoactive compounds to alter consciousness states, medicinal and recreational effects or access other psychedelic phenomena was present at humanity's beginnings, at least since the Neolithic period (SAMORINI, 2019). Through trial-and-fail tests, the first hominids gathered knowledge and experienced the use of a wide variety of psychedelic plants: opium poppy (*Papaver somniferum*), fly-agaric (*Amanita muscaria*) and ergot (*Claviceps* spp.) in the Old World and coca (*Erythroxylum* spp.), Cocoa (*Theobroma cacao*) and mate (*Ilex paraguariensis*) in the New World (SAMORINI, 2019). The religious aspect of the use of psychoactive compounds is also common in early prehistory, helping the development of belief systems in traditional societies (GUERRA-DOCE, 2015). The significant presence of psychedelics in human prehistory sometimes makes space for highly alternative hypotheses of human evolution, such as the Stoned Ape Hypothesis (MCKENNA, 1993). This very unusual and speculative theory in Terence McKenna's Food of the Gods book relates the use of psychedelics in early history with awakening of human cognition and adaptive advantages.

One of the most interesting psychedelic natural products is *N*,*N*-dimethyltryptamine (DMT), an amino acid derived alkaloid with a potent hallucinogenic effect, which is endogenous in several species, including *Homo sapiens* (JAMIESON *et al*., 2021). DMT was first identified and synthesized in 1931 by Richard Manske, a Canadian chemist (MANSKE, 1931); however it was only in 1946 when a Brazilian microbiologist, Oswaldo Gonçalves de Lima, discovered DMT in natural occurrence in plants such as *Mimosa hostilis* and tried to elucidate its molecular structure (SEPARATA DE ARQUIVOS DO I.P.A, 1946). In 1956, Stephen Szara tested DMT intramuscular doses in himself and found it to have a psychotic effect similar to that caused by LSD. Most consequential, Szara traced the relationship between DMT psychedelic effects with serotonin metabolism (SZARA, 1956).

In the 1990s, Rick Strassman and others conducted dose-response data studies for intravenously administered DMT in drug users to study hallucinogenic action. The gathered data conclusion indicated that not only may DMT be safely administered - although it is not possible to separate hallucinogenic effects from drug use - but also could be used as a

serotonergic probe of behavioral and neuroendocrine variables in psychiatrically ill patient studies (STRASSMAN; QUALLS, 1994; STRASSMAN *et al*., 1994). In 2016, Rick Strassman and Gallimore proposed a model, through target-controlled continuous infusion, to prolong and provide an immersive psychedelic state and to better study the DMT's brain effects since DMT is also endogenously produced in the pineal gland (GALLIMORE; STRASSMAN, 2016). Discussing Rick Strassman and Gallimore's study, David Nichols, in 2017, argued that for endogenously DMT to have a significant effect, it would need much more concentration in the brain, thus more DMT produced by the pineal gland (NICHOLS, 2017). Since then, the literature discusses the concentration and potential of DMT (BARKER, 2018; GLYNOS *et al*., 2023).

The beginning of the DMT's biosynthesis pathway follows a general two step-route psychoactive reaction: the decarboxylation of amino acids by an enzyme aromatic L-amino acid decarboxylase (AADC) followed by the functional group adding to the substrate (JAMIESON *et al*., 2021). The first step of DMT's mechanism, the decarboxylation of the L-trytophan by AADC forming tryptamine, is well described in the literature, however the molecular details of the adding of methyl groups to tryptamine is not fully elucidated. The proposed mechanism of the double-methylation is sometimes described as S_N2 -like (FONTECAVE; ATTA; MULLIEZ, 2004; ZHANG, J; ZHENG, 2016). However, more studies are needed to ascertain this, in which mechanistic theoretical electronic density arguments can be helpful.

The double-methylation step of DMT's biosynthesis is carried out by the enzyme indolethylamine-*N*-methyltransferase (INMT), in which the cofactor *S*-adenosyl-L-methionine (SAM) donates a methyl group to the tryptamine substrate (shown in Figure 1) (JAMIESON *et al*., 2021). Since it is still not yet possible to conduct electronic calculations of large systems, particularly macromolecules such enzymes, hybrid QM:MM ONIOM methods, which divides the system in different levels of theory, can be of great assistance (CHUNG *et al*., 2012).

Therefore, this study proposes to perform QM:MM ONIOM theoretical calculations in order to give electronic insights of the double-methylation reaction mechanism of human endogenous DM, with posterior analysis of the hybridization states of each reaction step and contributions from non-covalent interactions (NCI) in the energy barriers.

Figure 1. The double-methylation system. The INMT enzyme secondary structure and the SAM (yellow) cofactor and tryptamine (red) substrate shown with the cartoon and stick representation.

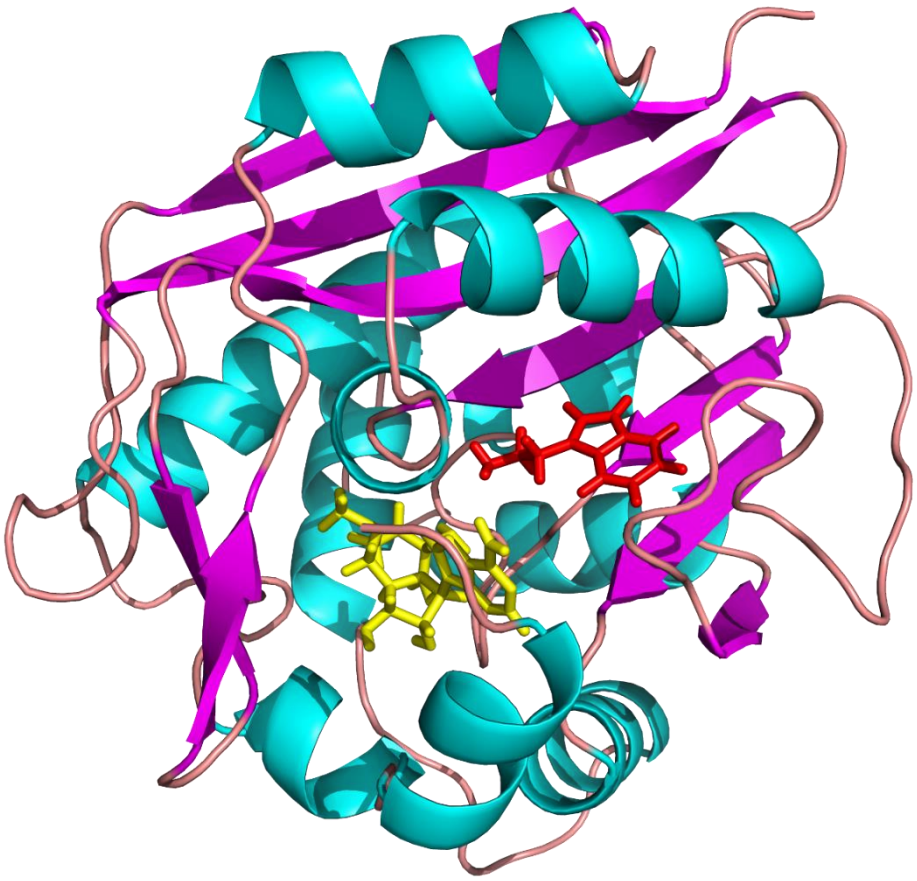

Source: author.

1.2 The pathway to propargylimine

Propargylimine ($HC \equiv C - CH = NH$, PGIM) is a nitrogen-bearing interstellar complex organic molecule (iCOM) (BIZZOCCHI *et al.*, 2020). Nitrogen-bearing iCOMs are interesting molecules in the interstellar medium (ISM) as they can be regarded as an primitive intermediate step towards the formation of amino acids and other biological building blocks of terrestrial life (APONTE *et al.*, 2017; BIZZOCCHI *et al.*, 2020). It's recent detection in the G+0.693-0.027 molecular cloud attracted attention, since PGIM's iminic moiety ($R - CH = NH$) is highly reactive, resulting in different functional groups attached to the PGIM, forming possible amino acids (BIZZOCCHI *et al.*, 2020).

The reaction mechanism of PGIM is not elucidated, being not a consensus in the literature, and although this imine iCOM has been recently discovery, only three studies were done with PGIM. In Lupi and collaborators study, a possible mechanism is proposed with the addition of the $\cdot C_2H$ radical to methanimine (CH_2NH) (LUPI; PUZZARINI; BARONE, 2020). Concepción *et al*., proposed an one-step isomerization kinetics model to describe the E/Z isomer ratio of PGIM and other imine-like molecules, demonstrating that the ratio strongly depends upon the imines stabilities (CONCEPCIÓN *et al*., 2021). In McDowell and Arthurs study, theoretical MP2 and DFT calculations were performed to binary dyads of PGIM with HF/H_2O complexes, founding PGIM hydrogen bonding to be predominantly at four different atoms and differing in the E/Z isomers (MCDOWELL; ARTHURS, 2022).

Bizzocchi *et al* proposed several mechanisms models for the synthesis of PGIM, from cyanoacetylene ($HC \equiv C - C \equiv N$) hydrogenation to acrylonitrile ($NC - CH = CH_2$) tautomerism (BIZZOCCHI *et al*., 2020). One mechanism model is the condensation reaction of propynal ($HC \equiv C - COH$) and ammonia (NH_3), followed by water elimination. In the ISM, amino acid precursors can be generated photochemically in reactions between nitriles and ammonia or through a Strecker-type mechanism that involves the condensation of ammonia and an aldehyde, close to the Bizzocchi *et al* propynal and ammonia mechanism proposal (RIMOLA *et al*., 2009; DANGER *et al*., 2011). Besides, the environment in which ISM reactions occur is of stark importance, with possible reactions happening in different sites, such as in the gas phase or ice sheet grains (SANDFORD *et al*., 2020). ISM chemical reactions can occur in gas phase process (Figure 2, top): ionization, dissociation and two-body reactions; and grain process (Figure 2, bottom): ice, silicate and organic sheets.

Thus, in the present work, is proposed a computational study of the mechanism model for the ISM formation of PGIM based on a Strecker-type synthesis of propynal with ammonia.

Since PGIM was first identified in the G+0.693-0.027 molecular cloud and other biologically-like molecules also react in the ISM, the proposed reaction adopted environment was the gas phase (SANDFORD *et al*., 2020). Also, the presence of glycine amino acid at the coma the 67P/Churyumov–Gerasimenko comet, suggests that iCOMs may react in cold environments and probably in the absence of water (BIZZOCCHI *et al*., 2020; ALTWEGG *et al*., 2016).

Figure 2. Possible environments in which propynal and ammonia Strecker mechanism may happen in the ISM: gas phase and ice sheet grains reactions.

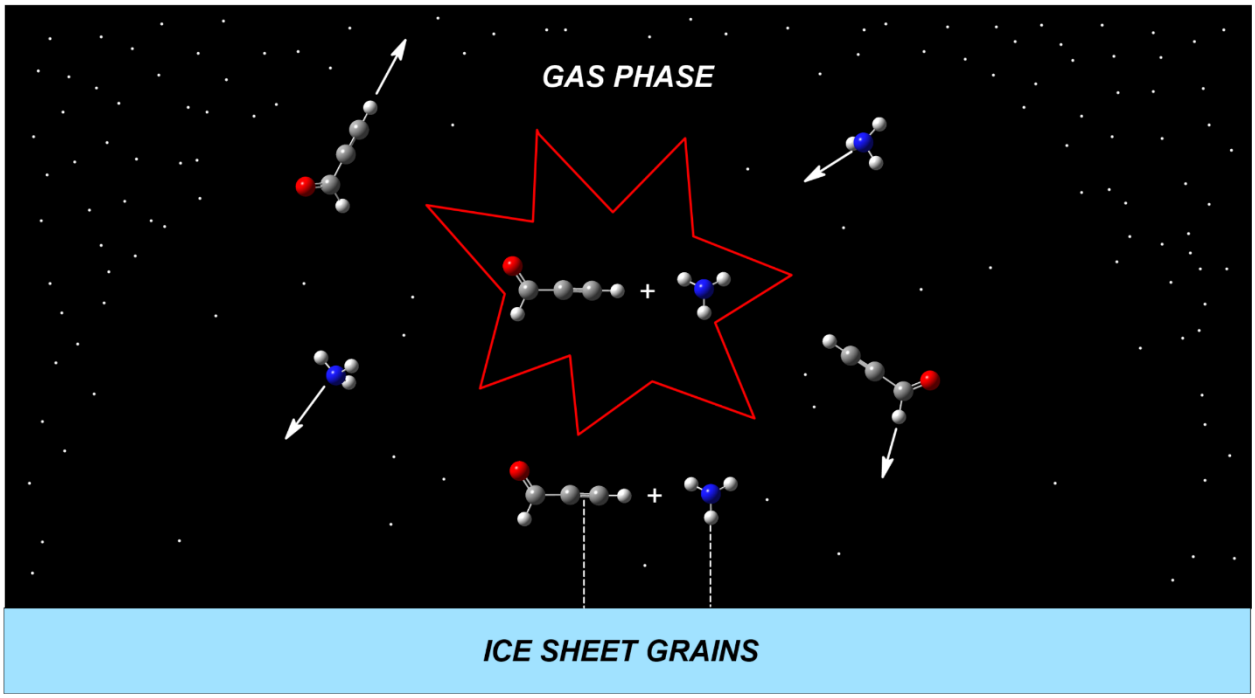

Source: author.

Density Functional Theory (DFT) calculations, with the wB97XD/aug-cc-pVTZ level of theory, were performed in order to obtain electronic data to build the Potential Energy Surface (PES) of the two-step PGIM mechanism, with hybridization states also analysed (ANSLYN; DOUGHERTY, 2006; FRISCH *et al*., 2009). Additionally, Quantum theory of Atoms (QTAIM) calculations were done to study the electron charge distribution of the reaction system in terms of (ρ), Laplacian of electronic density ($\nabla^2\rho$), ellipsity (ε) and electron localization function (ELF) (η) (BADER, 1991).

Part I

A MECHANISTIC INSIGHT FOR THE BIOSYNTHESIS OF *N*,*N*-DIMETHYLTRYPTAMINE: AN ONIOM THEORETICAL APPROACH

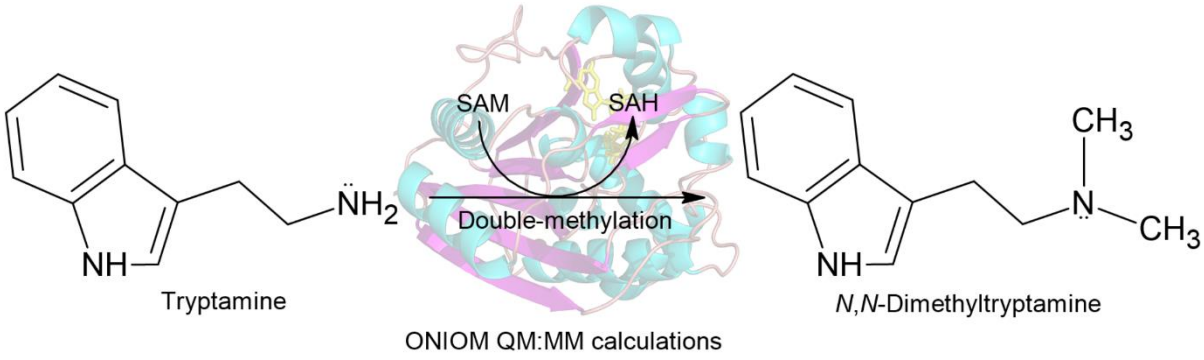

The elucidation of the double-methylation reaction route mechanism of tryptamine to biosynthesize *N*,*N*-dimethyltryptamine (DMT) through theoretical studies with and hybrid method approach.

RESUMO

Produtos naturais psicoativos são potentes agonistas serotoninérgicos capazes de modular funções cerebrais como memória e cognição. Essas substâncias têm mostrado potencial terapêutico para o tratamento de diversos transtornos mentais. O fato de a *N*,*N*-dimetiltriptamina (DMT) ser produzida endogenamente em várias plantas e animais, incluindo humanos, torna-a particularmente atraente. Como um alcaloide derivado de aminoácidos, a via biossintética da DMT faz parte da cascata bioquímica do L-triptofano e pode ser dividida na descarboxilação por uma L-aminoácido descarboxilase aromática (AADC) para a formação de triptamina e a subsequente dupla metilação pelo indoletilamina-*N*-metiltransferase (INMT) através do cofator *S*-adenosil-L-metionina (SAM), um doador de metila. Ao contrário do mecanismo de descarboxilação do L-triptofano, os detalhes moleculares da dupla-metilação da triptamina não foram elucidados. Portanto, propomos um modelo *in silico* usando cálculos de dinâmica molecular (MD), índice de interação não covalente (NCI) e teoria funcional de densidade (DFT) com o nível teórico ONIOM QM:MM B3LYP/6-31+G(d,p): MM/UFF. Com base nos dados energéticos obtidos, a superfície de energia potencial (PES) indica um perfil de mecanismo S_N2, com a segunda barreira de energia de metilação sendo a etapa limitante com $\delta G^{\ddagger} = 14.34\ \text{kcal} \cdot \text{mol}^{-1}$ maior que a metilação anterior, de acordo com a análise NCI, mostrando interações mais repulsivas para o segundo estado de transição. Além disso, as informações de hibridização de cada etapa de reação fornecem detalhes geométricos sobre a dupla metilação.

Palavras-chave: *N*,*N*-Dimetiltriptamina (DMT), mecanismo, ONIOM, QM:MM, teoria funcional da densidade (DFT), superfície de energia potencial (PES), psicoativos.

ABSTRACT

Psychoactive natural products are potent serotonergic agonists capable of modulating brain functions such as memory and cognition. These substances have shown therapeutic potential for treating various mental disorders. The fact that *N*,*N*-dimethyltryptamine (DMT) is produced endogenously in several plants and animals, including humans, makes it particularly attractive. As an amino acid-derived alkaloid, the DMT biosynthetic pathway is part of the L-tryptophan biochemical cascade and can be divided into the decarboxylation by an aromatic L-amino acid decarboxylase (AADC) for tryptamine formation and the subsequent double-methylation by the indolethylamine-*N*-methyltransferase (INMT) through the cofactor *S*-adenosyl-L-methionine (SAM), a methyl donor. Unlike the decarboxylation mechanism of L-tryptophan, the molecular details of the double methylation of tryptamine have not been elucidated. Therefore, we propose an *in silico* model using molecular dynamics (MD), non-covalent interaction index (NCI) and density functional theory (DFT) calculations with the ONIOM QM:MM B3LYP/6-31+G(d,p):MM/UFF level of theory. Based on the obtained energetic data, the potential energy surface (PES) indicates an S_N2 mechanism profile, with the second methylation energy barrier being the rate-limiting step with $\delta G^{\ddagger} = 14.34\ \text{kcal} \cdot \text{mol}^{-1}$ larger than the previous methylation, following the NCI analysis showing more repulsive interactions for the second transition state. In addition, the hybridization information of each reaction step provides geometric details about the double-methylation.

Keywords: *N*,*N*-Dimethyltryptamine (DMT), mechanism, ONIOM, QM:MM, density functional theory (DFT), potential energy surface (PES), psychoactives.

2.1 Introduction

The study of psychedelia phenomena in formal science is recent, particularly the investigation of the chemistry of the molecules behind psychedelic experiences. A boom in the discovery of new psychoactive compounds in the 1950s, such as lysergic acid diethylamide (LSD) and mescaline, caused psychologists and psychiatrists to try to use such psychedelics for psychotherapies. However, public misunderstanding and growing stark anti-drug legislation made any research progress difficult.[1,2] In the last two decades mainly, subtle changes in legislation and the social demand to deal with problems related to mental health have enabled the resurgence of scientific research with psychedelics. The results have attested to the safety and therapeutic benefits of these substances in clinical trials such as for treatment-resistant depression and post-traumatic stress disorder [3,4].

Currently, the research of psychoactive natural products explores the biological routes in which these molecules are synthesized in living organisms and has developed ways to synthesize such compounds for human use. Most isolated natural psychoactives originated from primary metabolites such as acetates, isoprenes, and amino acids, with the bulk of psychoactive compound precursors coming from amino acid derived alkaloids. Some examples are *N*,*N*-dimethyltryptamine (DMT), psilocybin, LSD and morphine.[5,6] In general, the biosynthesis of these molecules involves a two step-route: the decarboxylation of amino acids by an enzyme aromatic L-amino acid decarboxylase (AADC) followed by the functional group adding to the substrate. The most common group transfer reactions are methyl, prenyl and acetyl catalyzed by methyltransferases, prenyltransferases and acetyltransferases, respectively.[5]

The DMT is distinctly attractive, since it is widely produced endogenously in several species of plants and animals, such as *Psychotria viridis*, *Mimosa tenuiflora*, rodents and also present in humans.[7,8] In religious rituals of indigenous groups in the Amazonian rain forest and Santo Daime ceremonies, the traditional drink Ayahuasca is composed of two plants: *Banisteriopsis caapi* and *Psychotria viridis*, in which DMT is present in the latter.[9] DMT was first identified and synthesized in 1931 by Richard Manske,[10] however it was only in 1946 that Oswaldo Gonçalves de Lima, discovered its natural occurrence in plants such as *Mimosa hostilis*, a Jurema's constituent traditional drink, and tried to elucidate its molecular structure.[11] In order to verify DMT effects in humans, in 1956, Stephen Szára tested intramuscular doses and found it to have a psychotic effect similar to that caused by LSD and have symptoms such as hallucinations and euphoria. Most consequential, Szára traced the relationship between psychedelic effects with serotonin metabolism.[12] In the 1990s, Rick Strassman and others

conducted dose-response data studies for intravenously administered DMT in drug users to study hallucinogenic action. The gathered data conclusion indicated that this psychedelic could be used as a serotonergic probe in psychiatric patient studies.[13,14].

The precise function of endogenous human DMT is yet to be elucidated; nonetheless, a study associate DMT with the prevention of hypoxia.[15] Its biosynthesis in humans (Fig. 1) starts with the L-tryptophan; however, this amino acid is also the precursor of other molecules, such as serotonin and melatonin.[16] The enzymatic pathway of L-tryptophan (Fig. 1b), when it is hydroxylated by tryptophan hydroxylase, produces 5-hydroxytryptophan (5-HTP), which is then decarboxylated by AADC and generates serotonin (5-HT). Serotonin's acetylation by *N*-acetyl-transferase, followed by methylation of *N*-acetyl-5H by 5-hydroxyindole-O-methyltransferase, produces melatonin. Due to the structural similarities of DMT and melatonin, it has been proposed that the various dreaming states and even near-death experiences may be explained through elevated levels of endogenous DMT in these situations.[17,18]

The alternative route, the biosynthesis of DMT in humans (Fig. 1a), is the decarboxylation of L-tryptophan by AADC and tryptamine formation; and the double-methylation of tryptamine by the enzyme indolethylamine-*N*-methyltransferase (INMT) through the cofactor S-adenosyl-L-methionine (SAM), a methyl donor. The L-tryptophan decarboxylation mechanism is well elucidated in the literature;[5,19] however, the molecular details of the double methylation of tryptamine have not yet been described. The decarboxylation reaction route (Fig. 2) begins with the transaldimination of the AADC enzyme cofactor pyridoxalphosphate (PLP), in its aldimine reagent form, performed by L-tryptophan, forming a Schiff base and producing a PLP amino acid. Then the decarboxylation reaction occurs with the cleavage of the $C_\alpha - COO^-$ bond through an intermediate quinonoid formation reprotonated to undergo another transaldimination reaction, regenerating the aldimine reagent to its AADC enzyme and producing the next step substrate, tryptamine.

Thus, studies have been made to discover the reagents, intermediates and products of the double-methylation reaction route and new applications to the SAM/INMT transmethylation, however the literature does not describe the possible transition states of the reaction nor the energy barriers between one methylation to another.[20,21] Although the proposed double-methylation reaction mechanism is sometimes described as S_N2-like, more studies are needed to ascertain this, especially those with mechanistic electron-transfer energetic arguments.

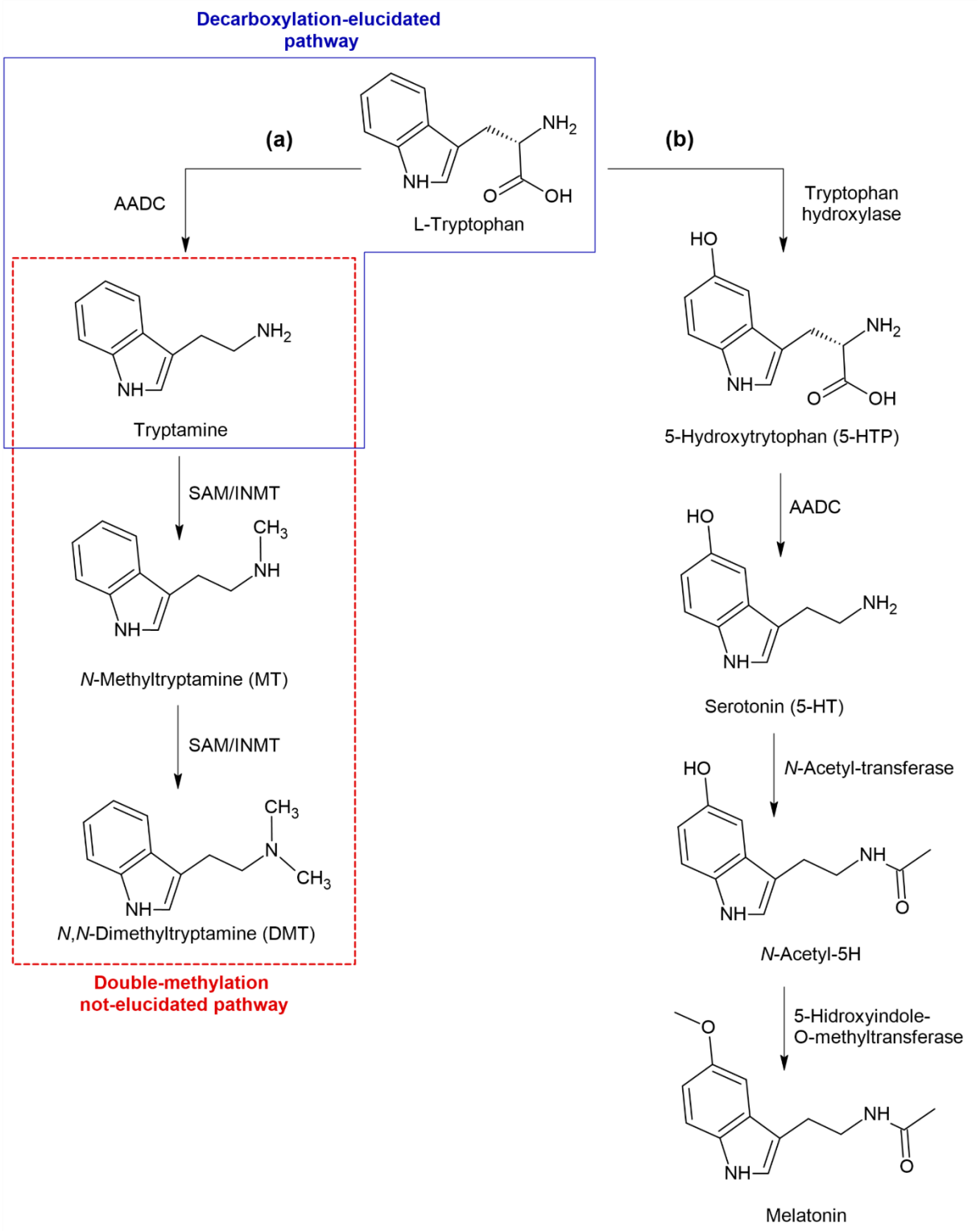

Fig 1. L-tryptophan biochemical cascade is divided into two routes: (a) decarboxylation (fully elucidated) and double-methylation (not-fully-elucidated) to produce DMT, or (b) the hydroxylation and decarboxylation to produce serotonin (5-HT), followed by acetylation and methylation to produce melatonin.

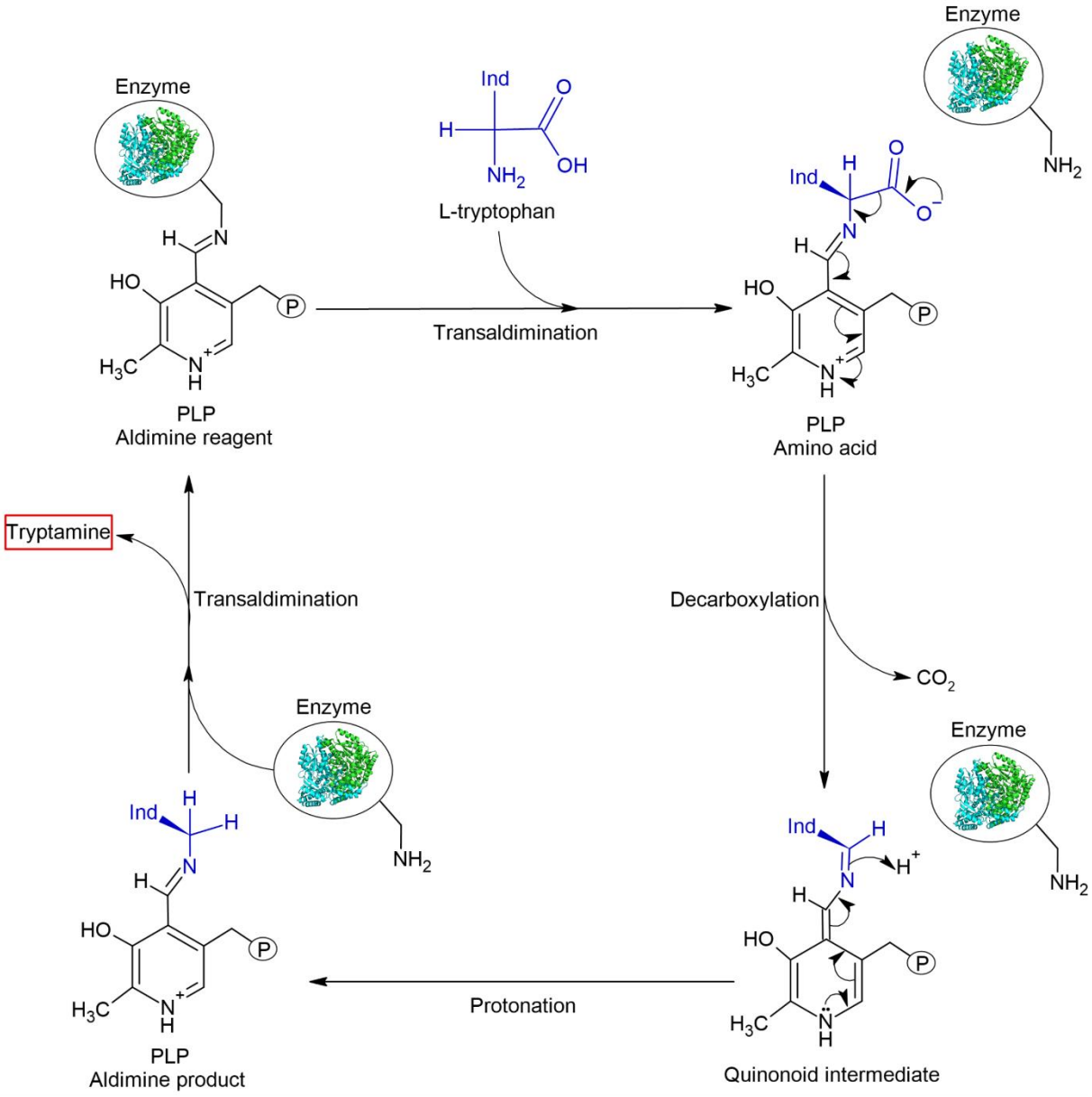

Fig 2. The mechanism of the decarboxylation elucidated reaction route and subsequent tryptamine formation. The *Ind* group is the bulk of L-tryptophan (indol + methyl group).

The described literature proposal mechanism (Fig. 1a) for the double-methylation reaction starts with the initial methylation of tryptamine by INMT's cofactor SAM to produce *N*-methyltryptamine (MT). Whether SAM's methyl group is restored through enzymatic processes by the INMT or another SAM/INMT performs the second methylation is a matter of debate. Then another methylation takes place, and DMT product is formed.

The first study to investigate DMT biosynthesis through a mathematical model or a numerical simulation was by Mack *et al* in 1988.[22] The study used kinetic data, obtained from

Phalaris aquatica, to show the conversion of tryptamine to DMT, the possible reaction intermediates and which methyltransferase is the most favorable to DMT biosynthesis. Only in 2014 did other studies explore this psychoactive using computational or theoretical methods. Nevertheless, they only investigated applications of this alkaloid or its interactions with molecules. Chu *et al*.[23] studied the Noncompetitive Inhibition of INMT by DMT and DMT-like compounds through molecular docking, and Öner *et al*.[24] studied conformational, spectroscopic and nonlinear optical properties of DMT through Density Functional Theory calculations.

Therefore, this study proposes using computational chemistry methods through a theoretical approach to give insights concerning the mechanism for the enzymatic reaction of human endogenous DMT biosynthesis. Employing computational calculations and simulations based on the density functional theory (DFT) and molecular dynamics (MD), the transition states of the double-methylation reaction route can be obtained, as well as the quantification of the energy barriers involved, and in addition, the elucidation of the mechanism of the ligand-receptor system, that can be accessed through ONIOM QM:MM calculations and later analysis of hybridization states and non-covalent interactions, with a theoretical proposed mechanism model. Since the current synthesis process uses non-environmentally friendly reagents, the molecular description of the enzymatic route could also support a green biotechnological process of large-scale exogenous production and help understand endogenous DMT levels in humans.

2.2 Materials and methods

2.2.1 System preparation

The structure of human INMT was obtained from crystallographic data in the Protein Data Bank (2A14 code), acquired by X-ray diffraction with resolution of 1.70 Å.[25] The water and sulfate cation molecules were deleted from the initial crystalline structure deposited in the database. Also, an S-adenosyl-L-homocysteine (SAH) molecule was present, the methyl-less byproduct of SAM's methylation, in which one methyl group was added to the sulfonium atom to obtain the SAM molecule.

In order to accommodate the tryptamine ligand into the INMT reaction active site, situated close to the SAM cofactor, was performed molecular dynamic simulations. The SAM topology parameters were obtained through acpype (AnteChamber PYthon Parser interfacE), an external tool program in the AmberTools program package,[26] in which parametrization

occurred with the AMBER99SB/AMBER99bsc0 merged force fields and using the bbc model to treat formal and partial charges.[26]

Furthermore, Gromacs 2020.4 was used to conduct molecular dynamics simulations with the INMT-SAM system.[27] Primarily, the geometry minimization energy step was done with the steepest descent algorithm,[28] followed by two 0.1-ns equilibration steps: a canonical NVT ensemble, with modified Berendsen V-rescale thermostat,[29] and an isothermic-isobaric NPT ensemble, with V-rescale thermostat and Parrinello-Rahman barostat,[30] to control the desired system temperature and pressure, respectively. The recommended TIP3P (transferable intermolecular potential with 3 points) water model was used to solvate the simulated system, and the system was neutralized by adding sodium counter ions. Concerning the MD simulation production, a modified NPT ensemble scheme was used to the dynamics with the Leap-Frog integrator to conduct a 100 ns simulation with a 2.0 fs time-step,[31] and implementing Amber03 force field.[32] The long-range interactions were modeled using PME (particle mesh Ewald) electrostatics with a cut-off of 1.0 nm, and LINCS was the constraint algorithm chosen. The before and after the production simulation step of the MD system is shown in Figure S1 in the Supporting Information. Afterward the MD simulation, the tryptamine ligand was introduced in the reaction active site of INMT at a distance of 6.2 Å of the sulfur atom of the SAM cofactor.

2.2.2 ONIOM layer construction and calculations

The ONIOM (Our own n-layered Integrated Molecular Orbital and Molecular Mechanics) method was developed to perform hybrid Quantum Mechanics and Molecular Mechanics (QM:MM) theoretical calculations.[33,34] Concerning this, it is still not yet possible to conduct electronic calculations of large systems, particularly macromolecules, with a high level of theory, then hybrid QM:MM calculations using the ONIOM method are of great assistance, since the partitioning of the system improves the calculation performance and time.[35-37]

Concerning a two-layered scheme, the ONIOM QM:MM approach divides the studied system into two parts: the model system, the QM treatment of the high-layer, and the real system, the MM treatment of both layers.[38] The targeted ONIOM energy (E_{ONIOM}) (Eq. 1) is the QM energy of the real system ($E_{QM,real}$), which is described as the sum of the QM model energy ($E_{QM,model}$) and the MM real energy ($E_{MM,real}$) subtracted from the MM model energy ($E_{MM,model}$), correcting the double-counted MM contribution.

$$E_{QM,real} \approx E_{ONIOM} = E_{QM,model} + E_{MM,real} - E_{MM,model} \quad (1)$$

Thus, the starting-point system, before the double-methylation reaction, is composed of two layers (Fig. 3a): (model layer) in which the double-methylation reaction is performed, and the low-layer (real layer), which is, all the reaction environment, the INMT enzyme.

Hence, in the initial step, the high-layer encompasses the SAM and tryptamine, containing 74 atoms. Since the chemical reaction will be performed at the model layer (Fig. 3b), the chosen level of theory for the DFT calculations was the hybrid Becke's three-parameter functional with the Lee-Yang-Parr correlation functional (B3LYP),[39,40] with the Gaussian Split-valence Pople's basis set 6-31+G(d,p). The mechanical embedding (ME) scheme was implemented to assist the ONIOM calculations, by treating electrostatic interactions in the QM:MM interplay.[38,41,42]

Concerning the low-layer, all the INMT enzyme environment was included. However, part of it was frozen (3720 atoms), and the other was set unconstrained (291 atoms) due to the extensive system (Fig. 3b). Both parts were treated with common MM Gaussian provided Universal Force Field (UFF) since they reside totally in the real model. The amino acid residues criteria to be set unconstrained was a cut-off radius of 6.5 Å around the sulfur atom (Fig. 3a), a slightly greater distance between tryptamine and SAM (6.2 Å), to confirm that tryptamine would be within this cut-off radius. The 12 chosen amino acid residues in the active site were: TYR11, PHE15, TYR20, TYR24, TYR25, LEU163, LEY164, ALA165, MET166, CYS168, TYR204 and VAL206.

The geometrical optimizations were carried out using the entire level of theory: ONIOM B3LYP/6-31+G(d,p):MM/UFF with the Gaussian 09 package.[43] Vibrational modes of the optimized geometries were calculated to determine whether the obtained geometries are true minima or transition states and to obtain the electronic energies necessary for the reaction mechanism understating. IRC (intrinsic reaction path) calculations were done to certify that the found transition states and products are indeed part of the reaction coordinate since the beginning reagents.

No implicit solvent model was added to the ONIOM system; the protein environment was then considered the sole solvent, with the high-layer interacting with the near-sided amino acid residues.

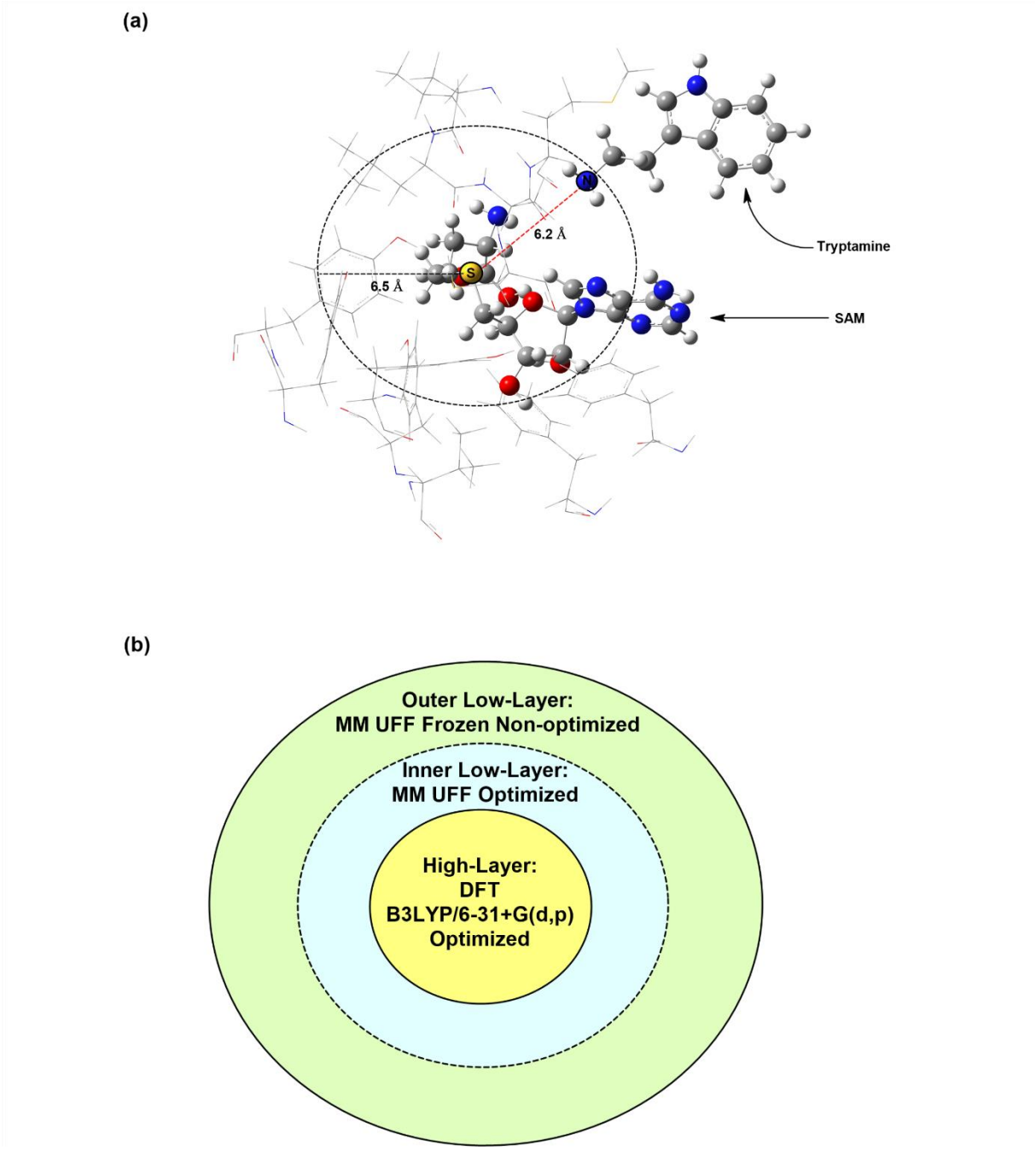

Fig 3. The studied QM/MM ONIOM system. (a) A depiction snapshot of the different system layers. The high and low-layers are depicted with the Ball and Bond Type and the Wireframe representations, respectively. (b) A diagram of the optimizations done in which layer in the QM/MM ONIOM system.

In addition to the obtained electronic energies, a validation of the energies was conducted as a matter of good practice.[37] In Eq. 2, the newly calculated electronic energy (EE_{sp}) was obtained through single-point calculations with a higher level of theory B3LYP-D3/6-

311++G(d,p), including Grimme D3 dispersion corrections included in the Gaussian 16 package,[44] and the Gibbs free energy correction ($G^{corr}_{opt-freq}$) is the same as the optimizations and frequency calculations with the lower basis set 6-31+G(d,p). This procedure verifies the scale of the energy difference between one basis set and another.

$$G^{total} = EE_{sp} + G^{corr}_{opt-freq} \quad (2)$$

2.2.3 NCI analysis

The non-covalent interaction index (NCI) is a study of weak interactions in 3D isosurfaces and 2D graph representations.[45] Besides the breaking and forming of covalent bonds, a myriad of interactions can also engage during chemical reactions, such as H-bonds, van der Waals interactions and steric effects. The NCI method uses the Reduced Density Gradient (RDG) (Eq. 3) to describe the deviation from electron density distribution $\rho(r)$, where $cs = 2(3\pi^2)^{1/3}$ and $\nabla\rho(r)$ is the first derivative of the electron density.[46]

$$RDG = \frac{|\nabla\rho(r)|}{cs\ \rho(r)^{4/3}} \quad (3)$$

The scale of interaction force comes from the created RDG isosurfaces, colored through the different system interactions. The RDG versus $\lambda_2\,\rho(r)$ graph, where λ_2 is the second highest eigenvalue of the $\rho(r)$ hessian matrix, displays the different non-covalent interactions, separating strong, attractive ($\lambda_2\,\rho(r) < 0$) and repulsive interactions ($\lambda_2\,\rho(r) > 0$), and mild interactions ($\lambda_2\,\rho(r) \approx 0$).[45]

After the double-methylation reaction, both transition states were analyzed for non-covalent interactions using Multiwfn 3.8 software.[47] The transition states were centralized at the SAH sulfur atom, the same as the ONIOM calculations, and the cut-off radius was 4.7 Å for both transition states (TS1 = 4.60 Å, TS2 = 4.64 Å) in order to ensure the reaction coordinate for TS1 (RNH_2-CH_3-SAH) and TS2 (RCH_3NH_2-CH_3-SAH) are considered in the NCI analysis. The sulfur atom surrounded amino acid residues was also included in the NCI analysis: TYR20, GLY63, GLY65, PHE86 and ALA164 for TS1, and GLY63, GLY65, PHE86, LEU164 and ALA165 for TS2.

2.2.4 Hybridization indices

The hybridization states (sp^n) of chemical species at each mechanism step can be quantified with a simple relationship (Eq. 4):

$$1 + n\,cos(\theta) = 0 \quad (4)$$

where θ is the mean angle of all the angles around the tryptamine, MT and DMT amine group nitrogen atom, and *n* is the hybridization index of the multiple hybridization states: sp^3, sp^2 and sp.[48]

2.3 Results and discussion

2.3.1 Boundary conditions of the calculations

We explored the mechanism of the double-methylation reaction route of tryptamine with INMT's cofactor SAM to elucidate the biosynthesis of DMT. The catalyzed methylation of amine-derived substrates, such as tryptamine by amino-N-methyltransferases, is well established in the literature,[49,50] being the INMT enzyme in charge of tryptamine's methylation.[51] Moreover, INMT's cofactor, SAM, is the second largest cofactor in the human body and the responsible methyl donor to the biosynthesis of DMT.[20] Previous studies have looked into a myriad of SAM applications, such as the rational biotechnological design of molecules since SAM can be the source for methylene, ribosyl, aminoalkyl and methyl groups.[21,52]

Through these facts, it is clear that the double-methylation is a SAM-dependent methyltransferase-catalyzed reaction. Besides, many SAM-methyltransferases react through an S_N2-like mechanism, and this could be the reaction pathway of the biosynthesis of DMT.[52] Therefore, the S_N2 mechanism was chosen to make our theoretical-computational model of the double- methylation reaction of tryptamine.

The protonated substrate state is a common feature of methyltransferase reactions.[53,54] However, with the protonated dominant form, the tryptamine's amine group is hindered from accepting a SAM's methyl group since the protonated tryptamine does not have a lone pair of electrons available, losing the behavior of a nucleophile and making the double-

methylation reaction impeded. Despite that, a computational study was done by Zhang *and* collaborators,[53] with SET-domain enzymes such as the protein-Lys-NH_2 (SET7/9) inquiry how such enzymes, in the protonated state (protein-Lys-NH_3^+), could be methylated by SAM cofactor. The authors discussed the possible use of water channels to escape the substrate proton to the aqueous solvent. Non-amine substrates in methyltransferases, such as xanthosine, are also in protonated states.[54] Besides the protonated substrates, amine's tryptamine has to be deprotonated before the enzymatic reaction for the double-methylation to proceed. Thus, the neutral tryptamine was the adopted initial reaction state, inasmuch more computational and experimental studies are yet to be done to verify how tryptamine, in SAM-methyltransferases are deprotonated.

2.3.2 ONIOM calculations

The calculated energies of each reaction step and the corresponding energy barriers $\Delta G^{\ddagger}$ are grouped in Table 1. The obtained Gibbs free energies G^{total}, using the single-point electronic energy EE_{sp} with a higher level of theory B3LYP-D3/6-311++G(d,p), is for the first and second methylation ≈ 0.425% and 0.418%, respectively, more negative concerning the electronic energy $EE_{opt-freq}$ of the opt-freq calculations (Table S1).

Table 1. Energy calculations at the ONIOM QM:MM B3LYP/6-31+G(d,p):MM/UFF level of theory. Using single-point energies EE_{sp} with a higher level of theory B3LYP-D3/6-311++G(d,p) the free Gibbs energies G^{total} were calculated with the $G^{total} = EE_{sp} + G^{corr}_{opt-freq}$ formula. The energy barriers $\Delta G^{\ddagger}$ are also listed.

Structure	$EE_{sp}/(\mathbf{E_h})$	$G^{corr}_{opt-freq}/(\mathbf{E_h})$	$G^{total}/(\mathbf{E_h})$	$\Delta G^{\ddagger}/(\mathbf{kcal \cdot mol^{-1}})$
$\mathbf{R1^{T}_{SAM}}$	-2173.297495	2.423495	-2170.874000	
$\mathbf{TS1^{T}_{SAM}}$	-2173.271723	2.428741	-2170.842982	19.463888
$\mathbf{P1H^{+MT}_{SAH}}$	-2173.330225	2.433038	-2170.897187	
$\mathbf{R2^{MT}_{SAM}}$	-2212.641881	2.452917	-2210.188964	
$\mathbf{TS2^{MT}_{SAM}}$	-2212.595960	2.460855	-2210.135105	33.796684
$\mathbf{P2H^{+DMT}_{SAH}}$	-2212.641572	2.462763	-2210.178809	

This verifies that the energy scale does not differentiate between one basis set and another of the same class, moreover serving as a validation to the obtained energy data.

The Gibbs free energy G^{total} profile of the two consecutive methylation reactions is represented in the Potential Energy Surface (PES) in Fig 4. The methylation reactions initiate at the change of substrate (the formation of tryptamine to MT, and MT to DMT), followed by the transition states and the protonated products. The Gibbs free energy profiles evidence that the change in substrate modifies the energy barrier $\Delta G^{\ddagger}$. The energy barrier difference concerning one methylation to another is $\delta G^{\ddagger} = 14.34\ \text{kcal} \cdot \text{mol}^{-1}$, being the second methylation the most energetic; this might be a result of the steric hindrance caused by the presence of the voluminous methyl group in the MT's amine, difficulting the second methylation, thus acquiring a higher energy barrier.[48] This energetic behavior reflects the Gibbs free energies of the products, making the protonated DMT more energetic than the protonated MT. Furthermore, besides the INMT enzyme having good affinities with a large variety of amine substrates, tryptamine seems to have the highest apparent turnover number, K_{cat}.[49] Therefore, the MT reagent in the second methylation might be affected by INMT kinetic preference.

A study conducted by Caldararu *et al*.[55] concerning the conversion of sulfite into sulfate by sulfite oxidase also used QM:MM computational methods. In this study, the coordination complex proposed enzymatic mechanism rate-limiting step has an energy barrier of $\approx 11\ \text{kcal} \cdot \text{mol}^{-1}$, regarded as a low value. However, other QM:MM studies implementing ONIOM and biochemically similar to the Tryp-SAM/INMT system have considerably higher energy barriers.

For instance, the PLP-dependent enzyme substrates, serine and tetrahydrofolate, in Santatiwongchai *et al*.[56] study, endures a retro-aldol synthetic process with a $16\ \text{kcal} \cdot \text{mol}^{-1}$ energy barrier, close to experimental results, $17 - 19\ \text{kcal} \cdot \text{mol}^{-1}$. In another study, tryptamine and DMT substrates were used to understand the oxidation mechanism of human trace amines. The rate-limiting energy barriers range from $16.8 - 32.5\ \text{kcal} \cdot \text{mol}^{-1}$ in the different proposed situations.[37]

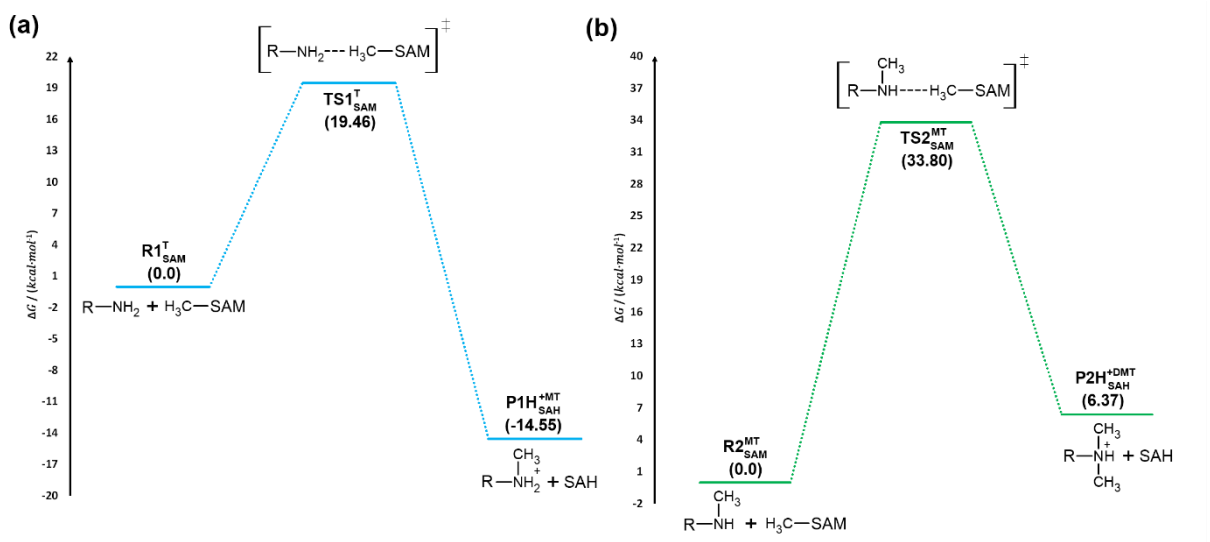

Fig 4. The Potential Energy Surface (PES) constructed with the free Gibbs energies G^{total} with EE_{sp} calculated with a higher level of theory B3LYP-D3/6-311++G(d,p). The energy barriers $\Delta G^{\ddagger}$ are shown for the double-methylation reaction route. The (a) blue and (b) green lines are the +MT and +DMT formation reaction coordinates, respectively.

The achieved energy barriers (the first and second transition states $\Delta G^{\ddagger} =$ 19.46 and 33.80 kcal $\cdot$ mol^{-1}, respectively) in the DMT biosynthesis are relatively similar to those found in other studies with near-reaction characteristics. For example, in Ntombela *et al.*,[57] they found rate-limiting energy barriers for the inhibition mechanism of D,D-carboxypeptidase with different *β*–lactam ligands range $16.62 - 30.29$ kcal $\cdot$ mol^{-1}, whereas in Sanusi *et al.*,[58] the energy barrier range of the hydrolyses inhibition mechanism of B and C-SA HIV-1 substrates, varies from $\approx 14 - 23$ kcal $\cdot$ mol^{-1}. respectively. Both aforementioned studies use the ONIOM method and propose concerted enzymatic mechanisms.

2.3.3 NCI analysis

The NCI data was gathered to study non-covalent interactions in both methylation reaction transition states. The used RDG isosurface value is 0.60, and the color scale data range is -0.02 to 0.02 $(sign\,\lambda_2\,\rho(r))$. In the obtained 3D NCI isosurfaces representation (Fig. 5), the observation of mild interactions is difficult due to the shown spatial distribution of interacting amino acid residues and the reactive system (Tryptamine or *N*-methyltryptamine, SAH cofactor and the transfer methyl group) isosurfaces in both transition states. However, the

obtained 2D NCI graph representation (Fig. 5), indicated by the RDG versus $\lambda_2\,\rho(r)$ black circle, shows more significant mild interactions, such as van der Waals interactions, for TS1 than for TS2.

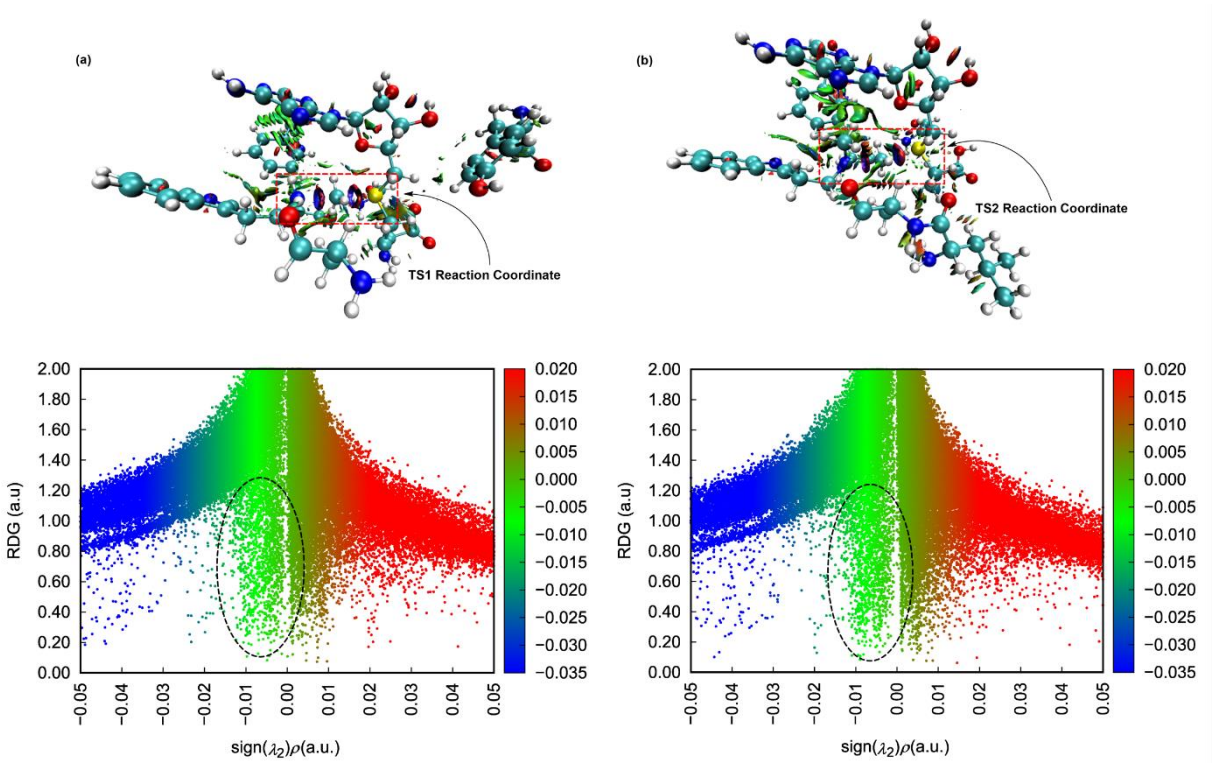

Fig 5. 3D isosurfaces and 2D graph NCI representations for the transition state of the (a) First methylation with the TS1 reaction coordinate (RNH_2-CH_3-SAH) highlighted and the (b) Second methylation TS2 reaction coordinate (RCH_3NH_2-CH_3-SAH) highlighted. The colors blue, red and green represent strong attractive and repulsive interactions, and mild interactions, respectively. The black circles represent the comparative mild interactions in both transition states.

Furthermore, the general observation of repulsive interactions, such as steric effects, in 2D NCI graphic representation in both transitional states seems similar. Nevertheless, the observation of the 3D NCI isosurfaces representations shows the TS1 reaction coordinate (Fig. 5a) to less repulsive interactions than the TS2 reaction coordinate (Fig. 5b), especially the more repulsive TS2 isosurface area close to the accepting nitrogen. This might be due to the presence of the methyl group in the TS2, thus complicating the methylation. Therefore, these results follow the obtained energy barriers since the difference concerning one methylation to another is $\delta G^{\ddagger} = 14.65\ \text{kcal} \cdot \text{mol}^{-1}$, with the second methylation being higher.

2.3.4 Hybridization analyses

The hybridization of the double-methylation reaction was also studied. Each reaction mechanism step: reagents, transition states and the final protonated products, was obtained the mean angle (θ) and hybridization index (n) of the amine group nitrogen atom of tryptamine, MT and DMT. At the beginning of the first methylation (Fig. 6a), the hybridization is $sp^{3.10}$, with an almost perfect tetrahedron arrangement (109.5°). Then, after the methyl group adding, the hybridization continues $\approx sp^3$, with a slight increase in the transition state ($sp^{3.24}$), due to the approximation of the chemical species. Notably, at the second methylation (Fig. 6b), the initial MT reagent has a hybridization of $sp^{2.40}$, close to the trigonal planar arrangement mean angle (120°).[48] The molecular geometry distortion, in both tryptamine and MT, is triggered by the lone pair of electrons in the amine nitrogen atom. Therefore, the MT arrangement might be explained by the lone pair weak perturbation in the electronic structure of MT, in contrast with tryptamine, and the presence of a newly added methyl group. Finally, the second methylation ends with an approximate tetrahedron arrangement ($sp^{3.02}$), also passing through an increase in the transition state ($sp^{2.76}$).

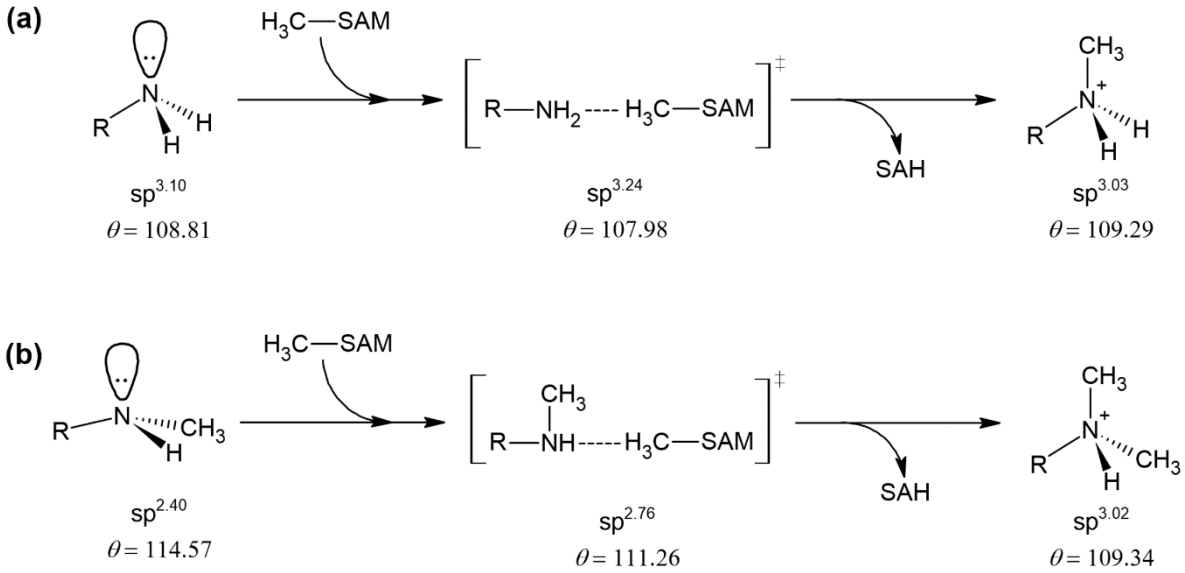

Fig 6. The hybridization analyses of the double-methylation reaction. The R group is the bulk of the tryptamine, MT and DMT structures. (a) The First methylation and the (b) Second methylation are shown with the obtained mean angle (θ) and hybridization index (n) of the amine group nitrogen atom for the reagents, transition states and the final protonated products.

2.3.5 Reaction mechanism

The PES (Fig. 4) represented profile of both methylations are *S_N2* based reactions, indicating a biomolecular reaction with each methylation taking place in a single reaction step through an unstable transition state.[48] Thus, based on the energetic calculated data, a mechanism of the double-methylation reaction of tryptamine with INMT's cofactor SAM of the biosynthesis of DMT was proposed.

The double-methylation reaction route initiates with the first methylation of tryptamine by SAM (Fig. 7a) through the attack of the lone pair of electrons to the methyl group of SAM and the MT intermediate formation with a $\Delta G^{\ddagger} = 19.46\ \text{kcal} \cdot \text{mol}^{-1}$ energy barrier, followed by its deprotonation. A 5.0 Å cut-off radius, centered on the N atom of both MT and DMT transition states, reveled the presence of THR162 and MET166 INMT amino acids, whose hydroxyl and thioether side-chains, respectively, could deprotonate the substrate hydrogen's. The strong electrophilic character of SAM is enhanced by the positively charged sulfonium, which renders its bonded methyl as a large leaving group.[21] In addition, the tryptamine amine group, acting as a nucleophile, is a strong base improving the *S_N2* reaction rate even further. Therefore, this demonstrates the favorable thermodynamics of SAM-dependent methyltransferase-catalyzed reactions.

The second methylation (Fig. 7b) occurs with the MT intermediate attacking the methyl group of another SAM cofactor, finally forming the *N*,*N*-dimethyltryptamine with a $\Delta G^{\ddagger} = 33.80\ \text{kcal} \cdot \text{mol}^{-1}$ energy barrier, followed by its deprotonation. The protonated DMT formation energy barrier $\delta G^{\ddagger} = 14.34\ \text{kcal} \cdot \text{mol}^{-1}$ is more considerable concerning the first methylation. This results from the methyl group presence in the MT reagent, impeding another methyl entrance; thus, the second methylation reacquires a larger energy barrier. Besides, secondary amines are weaker nucleophiles than primary ones.[48] Furthermore, the initial MT hybridization of $sp^{2.40}$, close to a trigonal planar arrangement, instead of tryptamine's tetrahedron arrangement ($sp^{3.10}$), might influence the acceptance of the second methyl group.[48] Thus, from the pooled results, the *S_N2* profile is the most plausible mechanism for the double-methylation, with the kinetics of the first methylation more favorable than the second one, due to the more significant energy barrier ($\Delta G^{\ddagger} = 33.80\ \text{kcal} \cdot \text{mol}^{-1}$), making the second methylation the rate-limiting step of the double-methylation reaction.

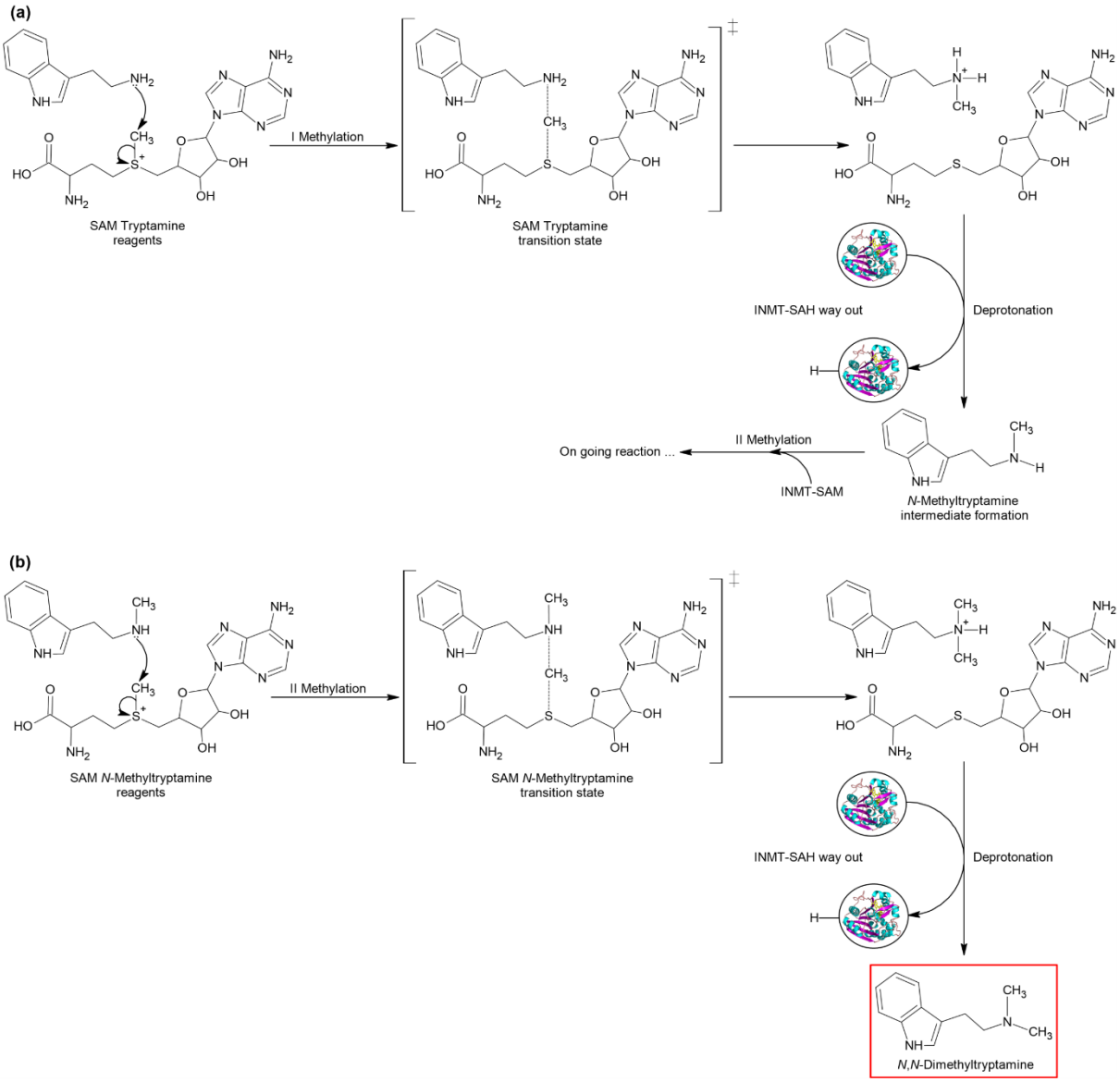

Fig 7. The proposed modeled mechanism of the double-methylation reaction route. (a) The first methylation of tryptamine and the MT formation and the (b) second methylation of MT and the DMT final formation, ending the mechanism.

In 2017, David Nichols discussed a previously proposed DMT study by Strassman and Gallimore concerning how to prolong the immersive psychedelic state of DMT via a target-controlled model.[59,60] Nichols argued that for endogenously DMT to have a significant effect, it would need more concentration in the brain; tryptamine, MT and DMT are found in trace quantities in the human body.[37] The explanation for the low concentration of DMT in the brain is still a matter of debate; however, in 2018, Steven Barker asserted that any speculation to

figure out DMT's endogenous role should be considered due to the lack of DMT brain studies in humans.[1] In a recent study, Glynos *et al*.[61] reported the non-essential presence of INMT for DMT biosynthesis in rat INMT and rat brain and lung tissue extracts. Nevertheless, human and rabbit INMT and rabbit lung tissue extracts are highly active in producing MT and DMT. Furthermore, it is stated that the sequence homology of INMT between humans and rabbits is quite close (89%), different from the sequence of mice (57%).

In Kubicskó and Farkas study, the oxidation mechanism of tryptamine and DMT by monoamine oxidase (MAO) was investigated through ONIOM calculations.[37] It was found that the energy barrier of DMT is lower than tryptamine, therefore strengthening the hypothesis that the low concentration of DMT might be caused by DMT synthesis followed by immediate oxidation. Another hypothesis could be the inhibition of INMT by DMT, limiting the synthesized amount of DMT through a self-regulated system.[62] A study conducted by Chu *et al*.[23] in 2014 (one of the first DMT computational studies) examined the noncompetitive inhibition of INMT by DMT through *in silico* molecular docking analyses and found INMT to be more inhibited by DMT than other amine-like molecules.

Therefore, in the present study, we investigated the double-methylation mechanism of Tryp to biosynthesize DMT through a model of two separate consecutive S_N2 reactions performed by ONIOM QM:MM calculations. It was found that the energy barrier difference between reactions is $\delta G^{\ddagger} = 14.34\ \text{kcal} \cdot \text{mol}^{-1}$, with the first methylation being regarded as the more thermodynamically favorable reaction. Thus, we hypothesize that the low DMT concentration in the brain is occasioned, in addition to other aforementioned causes, by the MT more considerable energy barrier, limiting the amount of DMT; being necessary to overcome this rate-limiting barrier, in another yet-to-be-considered way, to increase DMT concentration.

2.4 Conclusion

The present study explored the mechanism of the double-methylation reaction route of tryptamine to biosynthesize DMT. We investigated the DMT mechanism through MD simulation, NCI analysis and DFT calculations with the ONIOM QM:MM method using the B3LYP/6-31+G(d,p):MM/UFF level of theory in order to describe the influence of the energy barriers involved in the reaction course and also obtaining the transition states of both methylations. Thus, based on the energetic data, we aimed to give mechanistic insights of the biosynthesis of DMT. The built PES free Gibbs energy profiles of both methylations are of S_N2 reactions, with +MT and +DMT formations passing each one through a single bimolecular

reaction step. The energy barriers of the first and second methylations are $\Delta G^{\ddagger} = 19.46$ and $33.80\ \text{kcal} \cdot \text{mol}^{-1}$, respectively. The key finding is that the MT energy barrier is $\delta G^{\ddagger} = 14.34\ \text{kcal} \cdot \text{mol}^{-1}$ larger than the tryptamine energy barrier. This behavior is explained by the methyl group presence in the MT reagent impeding the second methyl donation, which agrees with NCI data indicating the first transition state to have less repulsive and more mild non-covalent interactions, and also the preference of the INMT enzyme for primary amines such as tryptamine, which are stronger nucleophiles than secondary amines. The obtained hybridizations of each reaction step provide information about the geometry details in the course of the mechanism. The significant change in hybridization at the initial MT reagent ($sp^{2.40}$) modifies the electronic arrangement influencing the second methylation acceptance of a methyl group. The gathered data evidence that the double-methylation mechanism of DMT is an *S*$_N$*2*-like reaction, with the second methylation having the more considerable energy barrier and being the rate-limiting step, thus receiving the larger INMT enzyme stabilization contribution. Furthermore, the second methylation higher energy barrier could be hypothesized as the reason, in addition to other causes, of low DMT human brain concentration, thus, being significant to overcome this rate-limiting barrier to increase the DMT amount.

Author Contributions

Lucas Pinheiro Coutinho: investigation, writing – original draft. Sérgio Ruschi Bergamachi Silva: writing – reviewing & editing. Pedro de Lima-Neto: resources, writing – reviewing & editing. Norberto de Kássio Vieira Monteiro: supervision, writing – reviewing & editing.

Conflicts of interest

There are no conflicts to declare.

Acknowledgments

The acknowledgments come at the end of an article after the conclusions and before the notes and references. The authors thank the National High-Performance Processing Center (CENAPAD) of the Federal University of Ceará (UFC) for providing computational resources.

This study was financed by the Brazilian agency Conselho Nacional de Desenvolvimento Científico e Tecnologico (CNPq) and Lucas Coutinho CNPq master's degree scholarship, process number: 160588/2021-9 and validity from 01/10/2021 to 30/09/2023.

Notes and references

1 S. A. Barker, *Front. Neurosci.*, 2018, 12, 1–17.

2 R. L. Carhart-Harris and G. M. Goodwin, *Neuropsychopharmacology*, 2017, 42, 2105–2113.

3 F. Palhano-Fontes, D. Barreto, H. Onias, K. C. Andrade, M. M. Novaes, J. A. Pessoa, S. A. Mota-Rolim, F. L. Osório, R. Sanches, R. G. dos Santos, L. F. Tófoli, G. de Oliveira Silveira, M. Yonamine, J. Riba, F. R. Santos, A. A. Silva-Junior, J. C. Alchieri, N. L. Galvão-Coelho, B. Lobão-Soares, J. E. C. Hallak, E. Arcoverde, J. P. Maia-de-Oliveira and D. B. Araújo, *Psychol. Med.*, 2019, 49, 655–663.

4 J. M. Mitchell, M. Bogenschutz, A. Lilienstein, C. Harrison, S. Kleiman, K. Parker-Guilbert, M. Ot'alora G., W. Garas, C. Paleos, I. Gorman, C. Nicholas, M. Mithoefer, S. Carlin, B. Poulter, A. Mithoefer, S. Quevedo, G. Wells, S. S. Klaire, B. van der Kolk, K. Tzarfaty, R. Amiaz, R. Worthy, S. Shannon, J. D. Woolley, C. Marta, Y. Gelfand, E. Hapke, S. Amar, Y. Wallach, R. Brown, S. Hamilton, J. B. Wang, A. Coker, R. Matthews, A. de Boer, B. Yazar-Klosinski, A. Emerson and R. Doblin, *Nat. Med.*, 2021, 27, 1025–1033.

5 C. S. Jamieson, J. Misa, Y. Tang and J. M. Billingsley, *Chem. Soc. Rev.*, 2021, 50, 6950–7008.

6 I. Ujvary, *Ann. Ist. Super. Sanita*, 2014, **50**, 12–27.

7 J. M. Saavedra, J. T. Coyle and J. Axelrod, *J. Neurochem.*, 1973, 20, 743–752.

8 T. M. Carbonaro and M. B. Gatch, *Brain Res. Bull.*, 2016, 126, 74–88.

9 H. Kaasik, R. C. Z. Souza, F. S. Zandonadi, L. F. Tófoli and A. Sussulini, *J. Psychoactive Drugs*, 2021, 53, 65–75.

10 R. H. F. Manske, *Can. J. Res.*, 1931, 5, 592–600.

11 Observações sobre "Vinho da Jurema" Utilizado pelos índios Pancarú de Tacaratú (Pernambuco), Separata de arquivos do i.p.a technical report, 1946.

12 S. Szára, *Experientia*, 1956, 12, 441–442.

13 R. J. Strassman and C. R. Qualls, *Arch. Gen. Psychiatry*, 1994, 51, 85–97.

14 R. J. Strassman, C. R. Qualls, E. H. Uhlenhuth and R. Kellner, *Arch. Gen. Psychiatry*, 1994, 51, 98–108.

15 A. Szabo, A. Kovacs, J. Riba, S. Djurovic, E. Rajnavolgyi and E. Frecska, *Front. Neurosci.*, 2016.

16 J. G. Dean, *Front. Neurosci.*, 2018.

17 J. C. Callaway, *Med. Hypotheses*, 1988, 26, 119–124.

18 J. G. Dean, T. Liu, S. Huff, B. Sheler, S. A. Barker, R. J. Strassman, M. M. Wang and J. Borjigin, *Sci. Rep.*, 2019, 9, 9333.

19 Nelson, D. L. and Cox, M. M. *Lehninger Principles of Biochemistry*. Artmed, New York, 2014.

20 J. Zhang and Y. G. Zheng, *ACS Chem. Biol.*, 2016, 11, 583–597.

21 M. Fontecave, M. Atta and E. Mulliez, *Trends Biochem. Sci.*, 2004, 29, 243–249.

22 J. P. G. Mack, D. P. Mulvena and M. Slaytor, *Plant Physiol.*, 1988, 88, 315–320.

23 U. B. Chu, S. K. Vorperian, K. Satyshur, K. Eickstaedt, N. V Cozzi, T. Mavlyutov, A. R. Hajipour and A. E. Ruoho, *Biochemistry*, 2014, 53, 2956–2965.

24 N. Öner, Ö. Tamer, D. Avcı and Y. Atalay, *Spectrochim. Acta Part A Mol. Biomol. Spectrosc.*, 2014, 133, 542–549.

25 H. M. Berman, *Nucleic Acids Res.*, 2000, 28, 235–242.

26 A. W. S. da Silva and W. F. Vranken, *BMC Res. Notes*, 2012, 5, 367.

27 D. Van Der Spoel, E. Lindahl, B. Hess, G. Groenhof, A. E. Mark and H. J. C. Berendsen, *J. Comput. Chem.*, 2005, 26, 1701–1718.

28 Arfken, G. W. H. H. F. , *Mathematical Methods for Physicists*, Elsevier, Waltham, 2013.

29 G. Bussi, D. Donadio and M. Parrinello, *J. Chem. Phys.*, 2007, 126, 014101.

30 M. Parrinello and A. Rahman, *J. Appl. Phys.*, 1981, 52, 7182–7190.

31 W. L. Jorgensen, J. Chandrasekhar, J. D. Madura, R. W. Impey and M. L. Klein, *J. Chem. Phys.*, 1983, 79, 926–935.

32 Y. Duan, C. Wu, S. Chowdhury, M. C. Lee, G. Xiong, W. Zhang, R. Yang, P. Cieplak, R. Luo, T. Lee, J. Caldwell, J. Wang and P. Kollman, *J. Comput. Chem.*, 2003, 24, 1999–2012.

33 S. Dapprich, I. Komáromi, K. S. Byun, K. Morokuma and M. J. Frisch, *J. Mol. Struct. THEOCHEM*, 1999, 461–462, 1–21.

34 L. W. Chung, H. Hirao, X. Li and K. Morokuma, *WIREs Comput. Mol. Sci.*, 2012, 2, 327–350.

35 T. Vreven, K. Morokuma, Ö. Farkas, H. B. Schlegel and M. J. Frisch, *J. Comput. Chem.*, 2003, 24, 760–769.

36 C. L. Firme, N. K. V. Monteiro and S. R. B. Silva, *Comput. Theor. Chem.*, 2017, 1111, 40–49.

37 K. Kubicskó and Ö. Farkas, *Org. Biomol. Chem.*, 2020, 18, 9660–9674.

38 L. W. Chung, W. M. C. Sameera, R. Ramozzi, A. J. Page, M. Hatanaka, G. P. Petrova, T. V Harris, X. Li, Z. Ke, F. Liu, H. Li, L. Ding and K. Morokuma, *Chem. Rev.*, 2015, 115 12, 5678–5796.

39 A. D. Becke, *J. Chem. Phys.*, 1992, 96, 2155–2160.

40 C. Lee, W. Yang and R. G. Parr, *Phys. Rev. B*, 1988, 37, 785–789.

41 F. Maseras and K. Morokuma, *J. Comput. Chem.*, 1995, 16, 1170–1179.

42 T. Vreven, K. S. Byun, I. Komáromi, S. Dapprich, J. A. Montgomery, K. Morokuma and M. J. Frisch, *J. Chem. Theory Comput.*, 2006, 2, 815–826.

43 Frisch, M. J., Trucks, G. W., Schlegel, H. B., Scuseria, G. E., Robb, M. A., Cheeseman, J. R., Scalmani, G., Barone, V., Mennucci, B., Petersson, G.A., Nakatsuji, H., Caricato, M., Li, X., Hratchian, H. P., Izmaylov, A. F., Bloino, J., Zheng, G., Sonnenberg, J. L., Hada, M., Ehara, M., Toyota, K., Fukuda, R., Hasegawa, J., Ishida, M., Nakajima, T., Honda, Y., Kitao, O., Nakai, H., Vreven, T., Montgomery Jr., J. A., Peralta, J. E., Ogliaro, F., Bearpark, M., Heyd, J. J., Brothers, E., Kudin, K. N., Staroverov, V. N., Kobayashi, R., Normand, J., Raghavachari, K., Rendell, A., Burant, J. C., Iyengar, S. S., Tomasi, J., Cossi, M., Rega, N., Millam, J. M., Klene, M., Knox, J. E., Cross, J. B., Bakken, V., Adamo, C., Jaramillo, J., Gomperts, R., Stratmann, R. E., Yazyev, O., Austin, A. J., Cammi, R., Pomelli, C., Ochterski, J. W., Martin, R. L., Morokuma, K., Zakrzewski, V. G., Voth, G. A., Salvador, P., Dannenberg, J. J., Dapprich, S., Daniels, A. D., Farkas, Ö., Foresman, J. B., Ortiz, J. V., Cioslowski, J., & Fox, D. J., Gaussian 09 (Revision A.02.), Gaussian, Inc., Wallingford CT, 2016.

44 S. Grimme, J. Antony, S. Ehrlich and H. Krieg, J. *Chem. Phys.*, 2010, 132, 154104.

45 E. R. Johnson, S. Keinan, P. Mori-Sánchez, J. Contreras-García, A. J. Cohen and W. Yang, *J. Am. Chem. Soc.*, 2010, 132, 6498–6506.

46 J. Contreras-García, R. A. Boto, F. Izquierdo-Ruiz, I. Reva, T. Woller and M. Alonso, *Theor. Chem. Acc.*, 2016, 135, 242.

47 T. Lu and F. Chen, *J. Comput. Chem.*, 2012, 33, 580–592.

48 Anslyn, E. V., & Dougherty, D. A., *Modern Physical Organic Chemistry*, University Science Books, Herndon, 2006.

49 J. Li, C. Sun, W. Cai, J. Li, B. P. Rosen and J. Chen, *Mutat. Res. Mutat. Res.*, 2021, 788, 108396.

50 S. Park, Y. Byeon, Y.-S. Kim and K. Back, *J. Pineal Res.*, 2013, 54, 139–144.

51 B. Torres, J. S. Tyler, K. A. Satyshur and A. E. Ruoho, *PLoS One*, 2019, 14, e0219664.

52 A. W. Struck, M. L. Thompson, L. S. Wong and J. Micklefield, *ChemBioChem*, 2012, 13, 2642–2655.

53 X. Zhang and T. C. Bruice, *Proc. Natl. Acad. Sci.*, 2008, 105, 5728–5732.

54 P. Qian, H.-B. Guo, Y. Yue, L. Wang, X. Yang and H. Guo, *J. Chem. Inf. Model.*, 2016, 56, 1755–1761.

55 O. Caldararu, M. Feldt, D. Ciloboc, M.-C. van Severen, K. Starke, R. A. Mata, E. Nordlander and U. Ryde, *Sci. Rep.*, 2018, 8, 4684.

56 J. Santatiwongchai, D. Gleeson and M. P. Gleeson, *J. Phys. Chem. B*, 2019, 123, 407–418.

57 T. Ntombela, A. Seupersad, S. Maseko, C. U. Ibeji, G. Tolufashe, S. I. Maphumulo, T. Naicker, S. Baijnath, G. E. M. Maguire, T. Govender, G. Lamichhane, B. Honarparvar and H. G. Kruger, *J. Biomol. Struct. Dyn.*, 2022, 40, 7645–7655.

58 Z. K. Sanusi, M. M. Lawal, T. Govender, S. Baijnath, T. Naicker, G. E. M. Maguire, B. Honarparvar and H. G. Kruger, *Phys. Chem. Chem. Phys.*, 2020, 22, 2530–2539.

59 D. E. Nichols, *J. Psychopharmacol.*, 2017, 32, 30-36.

60 A. R. Gallimore and R. J. Strassman, *Front. Pharmacol.*, 2016, 7, 211.

61 N. G. Glynos, L. Carter, S. J. Lee, Y. Kim, R. T. Kennedy, G. A. Mashour, M. M. Wang and J. Borjigin, *Sci. Rep.*, 2023, 13, 280.

62 L. P. Cameron and D. E. Olson, *ACS Chem. Neurosci.*, 2018, 9, 2344–2357.

Electronic Supplementary Information

Table S1. Energy calculations at the ONIOM QM:MM B3LYP/6-31+G(d,p):MM/UFF level of theory, without using single-point electronic energy EE_{sp}. The energy barriers $\Delta G^{\ddagger}$ are also listed.

Structure	$EE_{opt-freq}/(\mathbf{E_h})$	$G^{corr}_{opt-freq}/(\mathbf{E_h})$	$G^{total}/(\mathbf{E_h})$	$\Delta G^{\ddagger}/(\mathbf{kcal \cdot mol^{-1}})$
$\mathbf{R1^{T}_{SAM}}$	-2164.113301	2.423495	-2161.689806	
$\mathbf{TS1^{T}_{SAM}}$	-2164.085097	2.428741	-2161.656356	20.989975
$\mathbf{P1H^{+MT}_{SAH}}$	-2164.143116	2.433038	-2161.710079	
$\mathbf{R2^{MT}_{SAM}}$	-2203.434360	2.452917	-2200.981443	
$\mathbf{TS2^{MT}_{SAM}}$	-2203.385557	2.460855	-2200.924703	35.604520
$\mathbf{P2H^{+DMT}_{SAH}}$	-2203.434032	2.462763	-2200.971269	

Table S2. ONIOM QM:MM energy calculations input/output (gjf/log) file names at the B3LYP-D3/6-311++G(d,p) level of theory for the single-point Electronic Energy (EE_{sp}) and B3LYP/6-31+G(d,p) level of theory for the frequency Gibbs Free Energy Correction ($G^{corr}_{opt-freq}$) values.

Structure	Gaussian input/output file
$\mathbf{R1^{T}_{SAM}}$	sp/freq_R1_T_SAM.gjf/log
$\mathbf{TS1^{T}_{SAM}}$	sp/freq_TS1_T_SAM.gjf/log
$\mathbf{P1H^{+MT}_{SAH}}$	sp/freq_P1H_+MT_SAH.gjf/log
$\mathbf{R2^{MT}_{SAM}}$	sp/freq_R2_MT_SAM.gjf/log
$\mathbf{TS2^{MT}_{SAM}}$	sp/freq_TS2_MT_SAM.gjf/log
$\mathbf{P2H^{+DMT}_{SAH}}$	sp/freq_P2H_+DMT_SAH.gjf/log

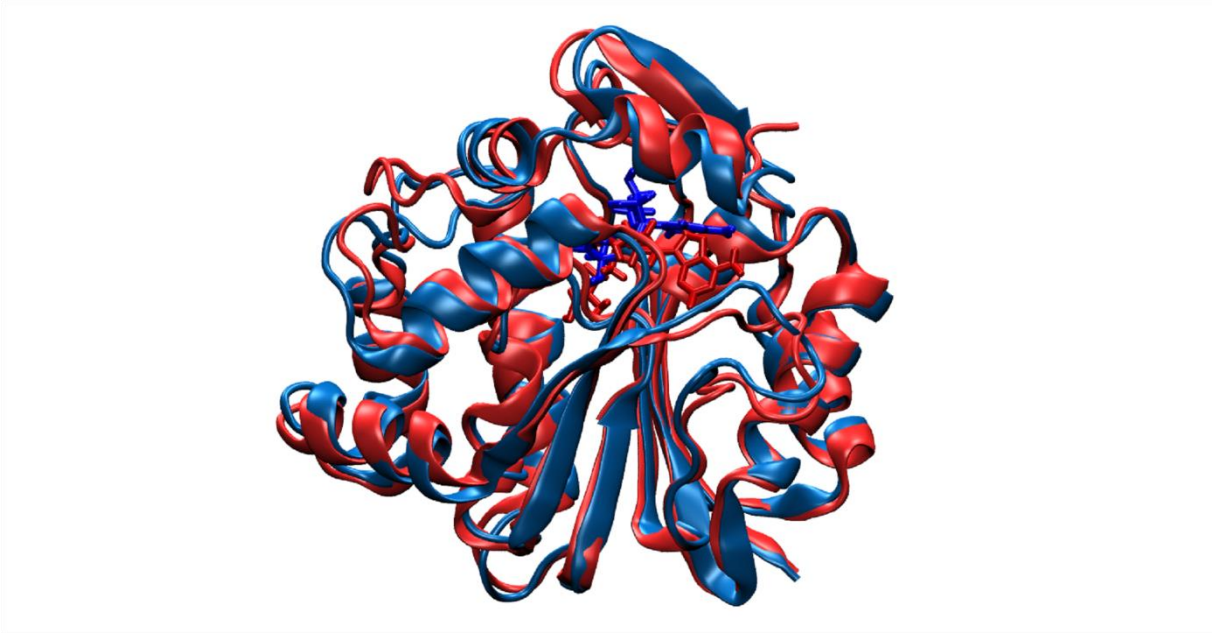

Fig S1. The aligned MD systems before (Red) and after (Blue) the production step. The INMT enzyme secondary structure and SAM ligand are shown as with the cartoon and stick representations, respectively.

Part II

A COMPUTATIONAL STUDY OF THE PROPARGYLIMINE (PGIM) FORMATION MECHANISM IN THE INTERSTELLAR MEDIUM (ISM)

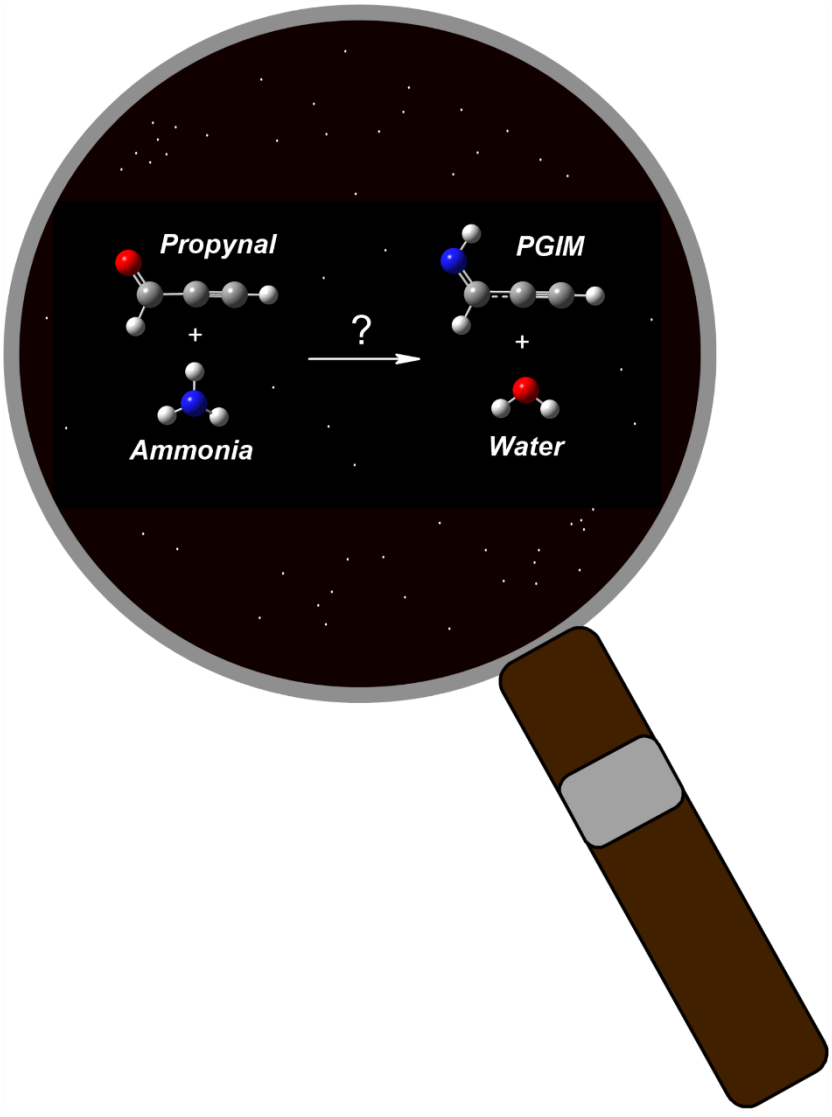

The theoretical study of the mechanism of propargylimine (PGIM) in the interstellar medium (ISM) following the Strecker synthesis.

RESUMO

Estudos teóricos de química quântica de mecanismos de reação envolvendo moléculas do meio interestelar (MI) são essenciais para entender a origem da matéria orgânica no ambiente espacial. Aqui, a química computacional foi usada para investigar a síntese de Strecker levando à formação da molécula interestelar propargilimina (PGIM). Nossa proposta para um mecanismo de síntese de PGIM em duas etapas envolveu o nível de teoria WB97XD/aug-ccpVTZ na fase gasosa em temperaturas de 10K e 298K. Com base nos dados energéticos, a Superfície de Energia Potencial (PES) indica um mecanismo S_N2 para a primeira etapa e um mecanismo E2 para a segunda etapa, com menor barreira de energia considerando a primeira etapa. Os resultados sugerem que o produto PGIM é termodinamicamente mais estável que os reagentes. Além disso, os dados topológicos de $\rho(r)$ e ε estão de acordo com os dados energéticos. Portanto, esses resultados demonstram que o PGIM pode ser formado através da síntese de Strecker em duas etapas em um possível ambiente interestelar.

Palavras-chave: Meio interestelar, PGIM, DFT, mecanismo.

ABSTRACT

Theoretical quantum chemistry studies of reaction mechanisms involving molecules of the interstellar medium (ISM) are essential to understand the origin of organic matter in the space environment. Here, computational chemistry was used to investigate the Strecker synthesis leading to the formation of interstellar molecule propargylimine (PGIM). Our proposal for a two-step mechanism of PGIM synthesis involved the WB97XD/aug-ccp-VTZ level of theory in the gas phase at temperatures of 10K and 298K. Based on the energetic data, the Potential Energy Surface (PES) indicates an S_N2 mechanism for the first step and E2 mechanism for the second step, with a lower energy barrier considering the first step. The results suggest that the PGIM product is thermodynamically more stable than the reactants. Furthermore, topological data from $\rho(r)$ and ε agree with the energetic data. Therefore, these results demonstrate that PGIM can be formed through two-step Strecker synthesis in a possible interstellar environment.

Keywords: Interstellar medium, PGIM, DFT, mechanism.

3.1 Introduction

The phenomenon of life is one of the most complex and ancient issues addressed by man. Identifying and studying molecules in the interstellar medium (ISM) plays a crucial role in increasing knowledge about chemical evolution and the formation of planets.[1,2] The intersection of areas such as astrochemistry and astrobiology is considered critical to understanding the connection of interstellar chemistry with circumstellar chemistry, encompassing the formation of simple molecules from atoms to the complexity of biological molecules. In the interstellar medium and circumstellar, 204 individual molecular species, consisting of 16 elements, were detected through astronomical observations.[3] Among these molecules, approximately 50 contain carbon and have 6 or more atoms, belonging to the class of the so-called interstellar complex organic molecules (iCOMs).[1] The iCOMs received enormous attention in the last decades, allowing how to elucidate the formation of relatively simple molecular structures to biochemically complex structures takes place.[4]

In the ISM, complex molecules are detected only in the densest sources. However, with one exception, even though iCOMs have only been found in the gas phase, there is strong evidence that they can form in ice sheets on interstellar grains.[5,6] For this reason, two alternative paradigms have emerged in the literature to explain their origin. One states that iCOMs are formed in the gas phase, and the other that iCOMs are synthesized on the surfaces of ice sheets, also called interstellar grains, in which reactants accumulate and diffuse to react. It is worth mentioning that these ice-covered grains catalyze important reactions on their surface.[7]

Glycine, also known as 2-aminoethanoic acid, is the simplest amino acid and is fundamentally involved in understanding the emergence of life, as it is intrinsically related to the formation of purines, nitrogenous bases involved in the formation of deoxyribonucleic acid (DNA).[8] This amino acid was discovered, jointly by methylamine and ethylamine, in the coma of the 67P/Churyumov–Gerasimenko comet through *in situ* mass spectrometry.[9] Although this has not yet been detected in the ISM, its discovery suggests a biochemical complexity in space which encourages us to elucidate the formation of prebiotic molecules. Furthermore, its presence suggests that the process capable of generating complex biochemical molecules can occur in cold environments and probably in the absence of water.[4]

Nitrogen-bearing iCOMs are particularly interesting as they can be regarded as an intermediate step towards the formation of biologically important species, such as amino acids,

considered the building blocks of all life on Earth, found in many biologically important species, including DNA, RNA, and proteins. Amino acids are the monomers of proteins and therefore are the primary targets in astrobiological studies, and their extraterrestrial origin is a widely discussed subject.

Many theoretical and experimental studies have investigated the chemical pathways and mechanisms that supposedly can culminate in synthesizing amino acids in the extraterrestrial environment.[10–13] In ISM, amino acid precursors can be generated photochemically in reactions between nitriles and ammonia[14] or through the Strecker mechanism that involves the condensation of ammonia and an aldehyde.[15]

Propargylimine (2-propyn-1-imine, $HC \equiv C - CH = NH$, PGIM) has a carbon nitrogen double bond, resulting in highly reactive amines capable of forming from the Strecker mechanism.[16] Different functional groups attached to the PGIM can result in a wide variety of amino acids.

Although PGIM has a structural isomer, acrylonitrile, well-studied species in the astrophysics field, the PGIM did not attract the attention of experimentalists, and few studies are present in the literature.[17] Since its discovery in 2020 by Bizzocchi *et al.*,[4] only three studies have been published on this imine.[13,18,19] In the study by Bizzocchi *et al.*, possible formation routes of the PGIM were presented.[4] One of these routes would be the reaction of propynal ($HC \equiv C - COH$) and ammonia (NH_3), followed by water elimination. However, there is still needs to be a consensus on the formation mechanism of the PGIM in the ISM.

In the context of astrochemistry, in recent years, theoretical studies have been devoted to investigating the possible chemical pathways that can lead to complex biological molecules in diverse extraterrestrial environments.[10–12,20,21] Foremost, Density Functional Theory (DFT) was used to calculate the geometrical structures and vibrational frequencies for all the stationary points included in the Potential Energy Surface (PES), namely, reactants, possible products, intermediates and transition states. Subsequently, Quantum Theory of Atoms in Molecules (QTAIM) calculations were used to examine the generated electron density distribution,[22] and hybridization states were analyzed in order to improve the PES reaction mechanism model.[23]

Based on these premises, we perform a state-of-the-art quantum-chemical characterization of stationary points on the $HC \equiv C - COH + NH_3$ reaction at two different temperatures (10K and 298K) to propose a PGIM synthesis pathway mechanism. No study

describing the chemical mechanism of PGIM synthesis through propynal and ammonia has been performed in the literature. Therefore, to study the mechanism of this reaction, we use the axiom of Strecker amino acid synthesis from the reaction of an aldehyde (propynal) with ammonia.[16]

3.2 Computational metodology

Theoretical calculations were performed using the Gaussian 09 suite of programs[24] with the level of theory at the wB97XD functional with empirical dispersion corrections,[25] and the aug-cc-pVTZ polarized triple-zeta basis set, augmented with added diffuse functions (AUG).[26] The calculations have been made with two temperatures, 10 and 298 K, in order to verify the difference between the optimized calculated energies, and the vacuum was applied to mimic the space ISM effect on the proposed mechanisms. The stationary points along the pathway leading to PGIM have been optimized, and the geometries were employed to perform harmonic vibrational frequencies calculations to determine the nature of each stationary point: minimum if all the frequencies are real and transition state if there is one, and only one, imaginary frequency. Saddle points have been assigned through Intrinsic Reaction Coordinates (IRC).[27,28]

Electron density was generated for later use in quantum theory of atoms in molecules (QTAIM) calculations, developed by Richard F.W. Bader and colleagues,[22,29,30] which seeks to define bonding using a topological analysis of the electron density distribution. All topological information of electronic density (ρ), Laplacian of electronic density ($\nabla^2\rho$), ellipsity (ε) and ELF (η) was obtained using Multiwfn version 3.8.[31]

The degree of ammonia nitrogen hybridization between the sp^2 and sp^3 states was quantified through the hybridization index (Eq. 1)[23] with the following equation:

$$1 + n\,cos(\theta) = 0 \qquad (1)$$

Where θ is the mean angle of three angles around the ammonia nitrogen atom.

3.3 Results and discussion

Although some studies have been conducted on water grains,[32,33] the contribution of gas phase chemistry cannot be neglected considering that there are often only small fractions of a chemical species in the ISM.[34] Although there is a rich interstellar chemistry, which occurs both in water grains and in the gas phase, we are still a long way from understanding all the chemical mechanisms. There is a dearth of information and only a small fraction of the elementary reactions have actually been adequately characterized. As a result, many models still miss crucial information on chemical species detected in space.

An important condition for the validation of the proposed mechanism, which starts from the condensation of ammonia with an aldehyde ($R-COH$), are the theoretical and experimental investigations based on the Strecker mechanism.[15,32] The propynal was detected towards G+0.693−0.027 molecular cloud and has an abundance of approximately $> 10^{-9}$.[4] As mentioned above, Bizzocchi and co-workers propose five formation routes of PGIM, where all proposals are based on molecular precursors that are more abundant than PGIM with the exception of the propynal precursor that is only marginally more abundant than PGIM. However, the lack of information about the associated reaction rates and energy barriers makes this route a great attraction for studying chemical reaction mechanisms that can lead to PGIM.

Based on these assumptions, the theoretical investigation of the PES to understand the formation mechanism of PGIM in the ISM, a two step reaction is proposed for its formation using propynal ($HC\equiv C-COH$) and ammonia (NH_3) (Eq. 2) to produce PGIM (Eq. 3) as follows:

$$HC\equiv C-COH+NH_3 \longrightarrow HC\equiv C-HCOH-NH_2 \quad (2)$$

$$HC\equiv C-HCOH-NH_2 \longrightarrow HC\equiv C-CH=NH+H_2O \quad (3)$$

The optimized geometries of reactants (**A**), products (**B**), intermediate (**I**) and transition states (**TS1**,**TS2**) are presented in Figure 1.

According to the modelled mechanism, the reaction between propynal and ammonia involves two steps: (i) formation of the intermediate aminoalcohol by condensation of propynal with ammonia (**1**-**2** in Figure 2); (ii) dehydration of this aminoalcohol and formation of 2-propyn-1-imine (PGIM) (**2**-**3** in Figure 2). The total energy (ΔE) and free energy (ΔG) for

each structure involved in the reaction between propynal with ammonia are listed in Table 1, while comparative ΔE and ΔG profiles are shown in Figure 3 and Figure 4 for the gas phase at 10K and 298 K temperature reactions, respectively.

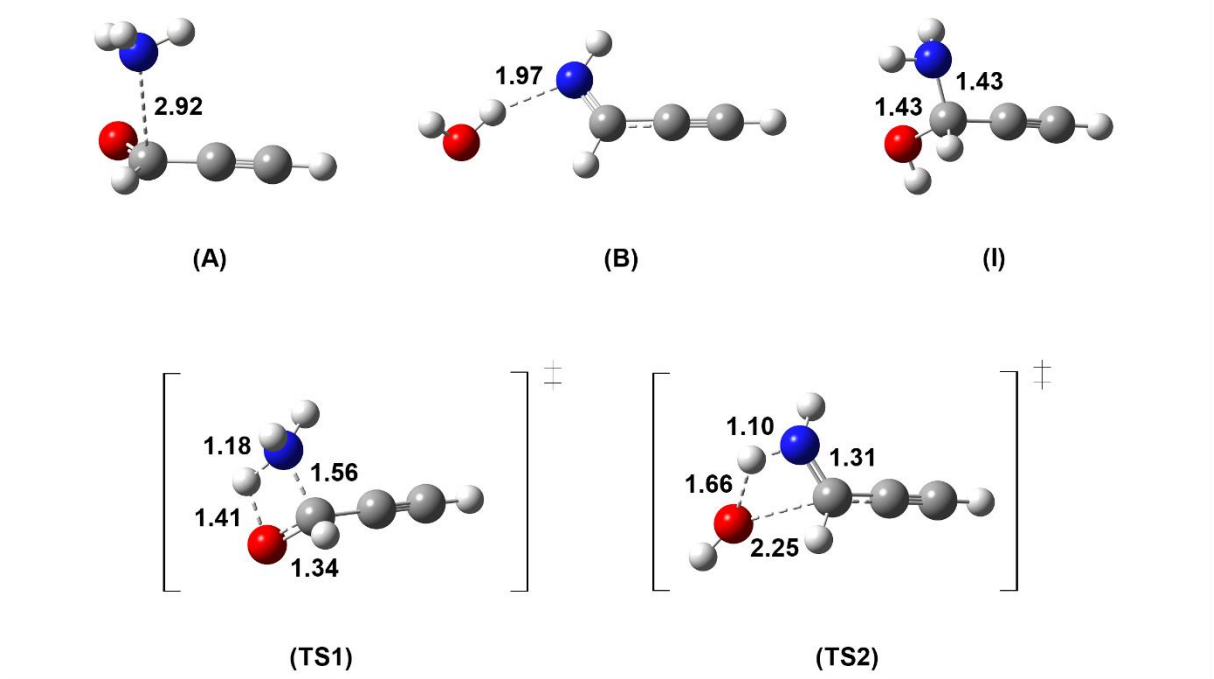

Fig 1. Optimized geometries for the reactants (**A**), products (**B**), intermediate (**I**) and transitions states (**TS1**,**TS2**). The units for bond lengths are in angstroms (Å).

The step-by-step description of the studied mechanism is thus detailed. Ammonia adds to propynal by a concerted nucleophilic attack of the N atom towards the carbonyl C atom and a proton transfer from NH_3 to the carbonyl O to give the intermediate aminoalcohol condensed propynal ($HC \equiv C - HCOH - NH_2$).[32] Starting from the reactants **1** (Figure 2) the condensation between NH_3 and $HC \equiv C - COH$ occurs through a transition state **TS1** with the development of a direct N-C bond and the proton transfer from NH_3 to $HC \equiv C - COH$. For this process the computed transition states $\Delta E^{\ddagger}$ and $\Delta G^{\ddagger}$ are 33.5902 and 33.7258 kcal $\cdot$ mol^{-1}, respectively, for the 10 K gas phase reaction (Figure 3) with the intermediate $HC \equiv C - HCOH - NH_2$ (**2**) being -7.8513 (ΔE) and -4.6975 (ΔG) kcal $\cdot$ mol^{-1} lower in energy than **1**.

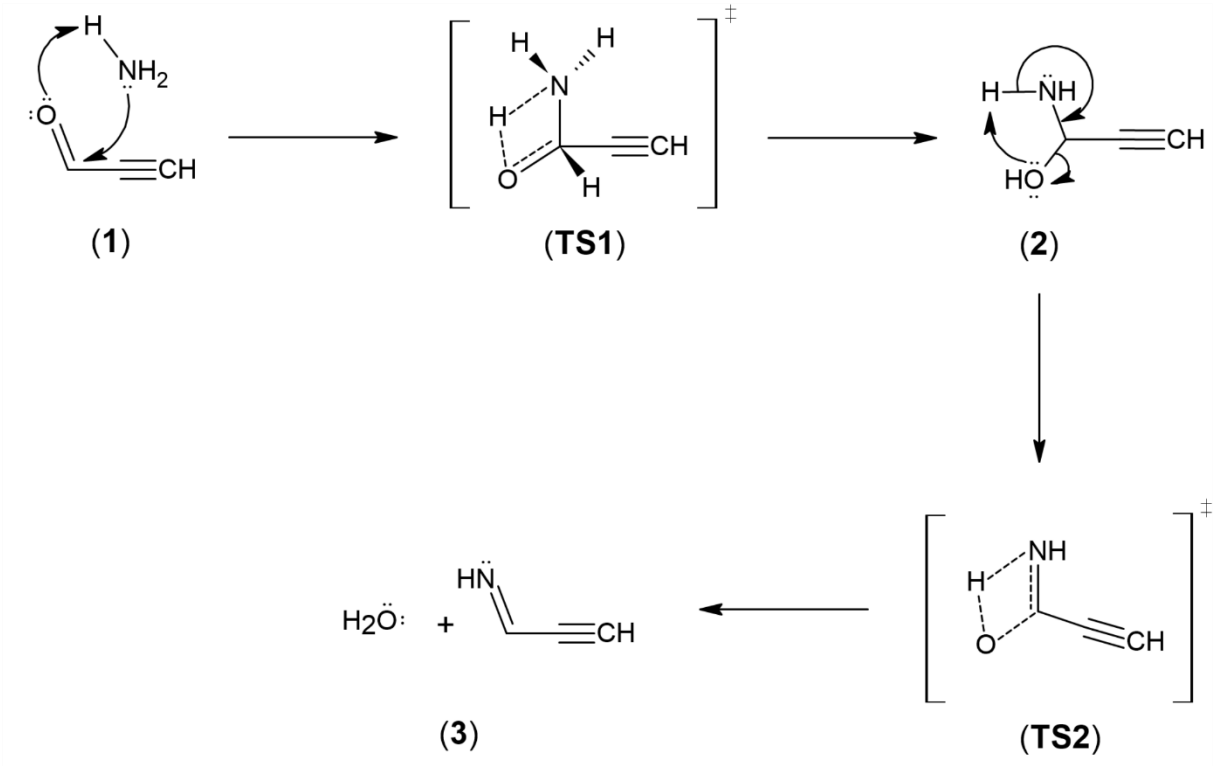

Fig 2. Schematic representation of the reaction mechanism of propynal with ammonia. The condensation (**1**-**2**) and dehydration (**2**-**3**) steps.

Table S1. Total electronic energy (ΔE) and free Gibbs energy (ΔG) in the gas phase model, with the ISM[a] (10 K) and room[b] (298 K) temperatures, for each of the structures in the reaction path obtained from the standard thermochemistry calculation at the level of theory WB97XD/aug-cc-pVTZ level of theory.

Structure	$\Delta E^a/(\mathbf{kcal \cdot mol^{-1}})$	$\Delta G^a/(\mathbf{kcal \cdot mol^{-1}})$	$\Delta E^b/(\mathbf{kcal \cdot mol^{-1}})$	$\Delta G^b/(\mathbf{kcal \cdot mol^{-1}})$
$\mathbf{R1^{NH_3}_{Prop}}$	0.0000	0.0000	0.0000	0.0000
$\mathbf{TS1^{NH_3}_{Prop}}$	33.5902	33.7258	39.5022	41.5369
$\mathbf{I_{C-Prop}}$	-7.8513	-4.6975	-6.5192	-1.3253
$\mathbf{TS2_{C-Prop}}$	46.6636	46.8889	59.6883	58.2072
$\mathbf{P^{H_2O}_{PGIM}}$	-1.6673	-0.9770	-1.9666	-0.0213

Considering the 298 K gas phase reaction, the condensation between NH_3 and $HC \equiv C - COH$ results in energy barriers of 39.5022 ($\Delta E^{\ddagger}$) and 41.5369 kcal · mol^{-1} ($\Delta G^{\ddagger}$) for **TS1** (Figure 4), with $HC \equiv C - HCOH - NH_2$ (**2**) being -6.5192 (ΔE) and -1.3253 kcal · mol^{-1} (ΔG) lower in energy than **1**.

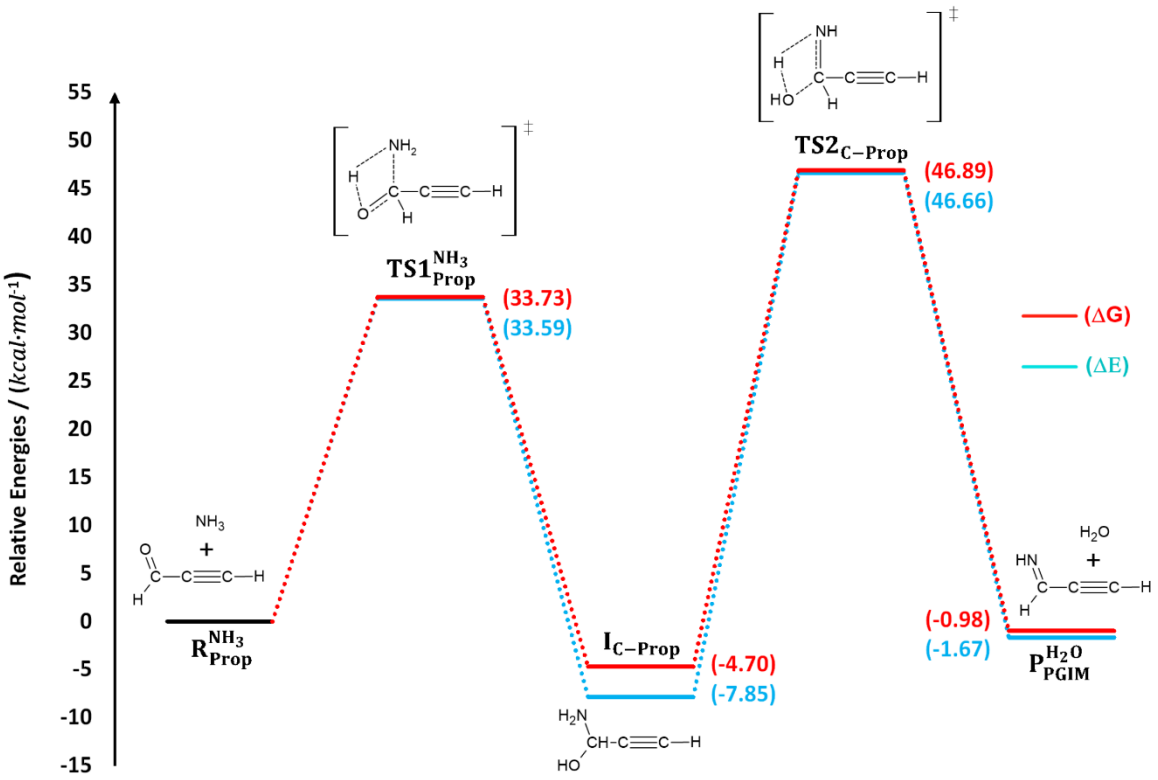

Fig 3. Free energy (ΔG) and total energy (ΔE) profile for the temperature of 10 K in gas phase model reaction between propynal and ammonia.

In the second step an E2 intramolecular reaction is performed with the intermediate condensed propynal ($HC \equiv C - HCOH - NH_2$). Beginning with the aminoalcohol (**2**), the hydroxyl abstract an hydrogen atom from the amine group, concurrently the N-C bond becomes a double bond occurring through a transition state **TS2** eliminating a water molecule and forming PGIM ($HC \equiv C - CH = NH$) (**3**). For this process the computed transition states $\Delta E^{\ddagger}$ and $\Delta G^{\ddagger}$ are 46.6636 and 46.8889 kcal · mol^{-1}, respectively, for the 10 K gas phase reaction (Figure 3) with the products $HC \equiv C - CH = NH + H_2O$ (**3**) being -1.6673 (ΔE) and -0.9770 (ΔG) kcal · mol^{-1} lower in energy than **1**.

Relating the 298 K gas phase reaction, the intramolecular elimination reaction $HC \equiv C - HCOH - NH_2$ results in energy barriers of 59.6883 ($\Delta E^{\ddagger}$) and 58.2072 kcal · mol^{-1} ($\Delta G^{\ddagger}$) for **TS2** (Figure 4), with $HC \equiv C - CH = NH + H_2O$ (**3**) being -1.9666 (ΔE) and -0.0213 kcal · mol^{-1} (ΔG) lower in energy than **1**.

From the $\Delta E^{\ddagger}$ and $\Delta G^{\ddagger}$, it can be seen that the energy barriers for the **TS1**, **TS2** have lower values for the studied mechanism considering 10 K than the 298 K temperature, thus the gas phase low temperature reaction model truly mimics the ISM effect on the proposed mechanisms. A possible explanation for the difference of energetic barriers with the 10 K gas phase model will be given through QTAIM analysis. The molecular graphs obtained through QTAIM analysis for **TS1** and **TS2** are shown in Figure 5 along with several topological data of selected bond critical points. Electronic density, $\rho(r)$, Laplacian of the electron density, $\nabla^2\rho(r)$, Ellipticity of electron density, ε, and Electron localization function η values are shown for bond critical points between atoms for the studied transition state structures.

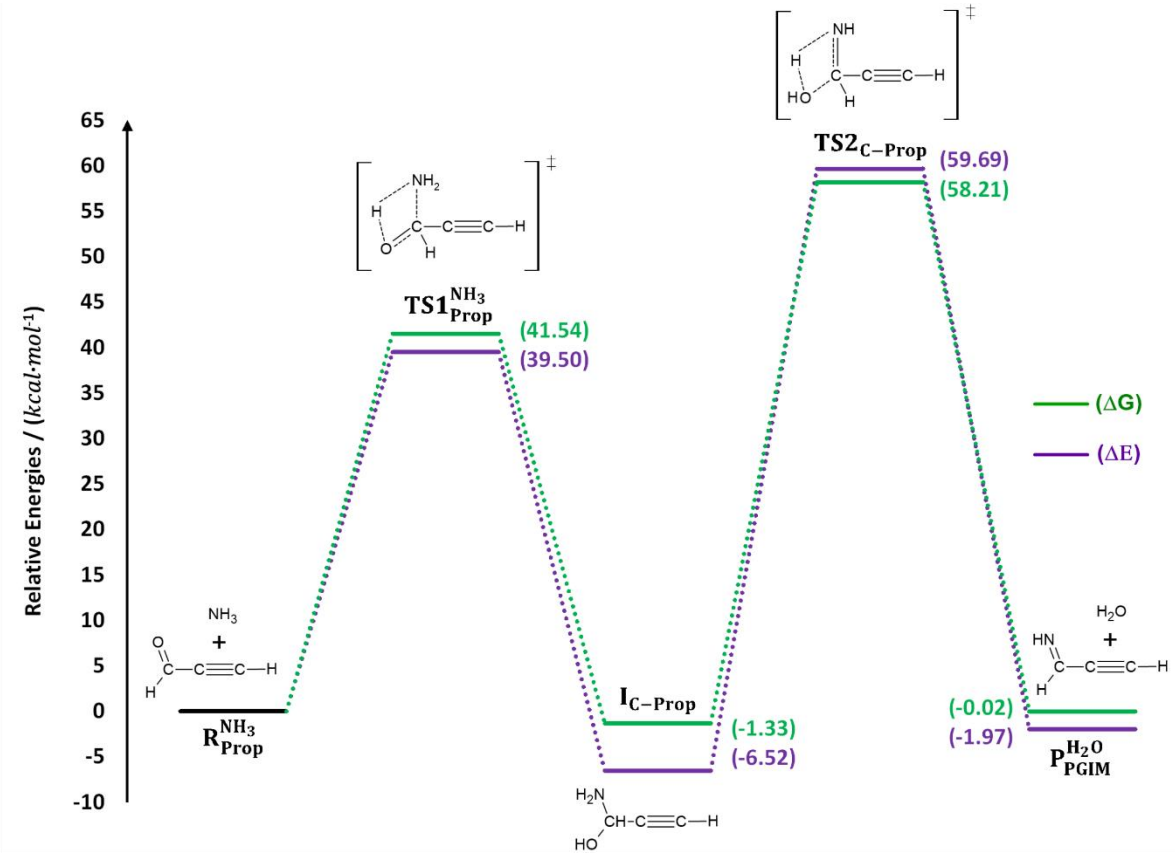

Fig 4. Free energy (ΔG) and total energy (ΔE) profile for the temperature of 298 K in gas phase model reaction between propynal and ammonia.

Considering the structure of the transition states (Figure 5), we can see that the **TS1** has a higher sum of $\rho(r)$ than the **TS2**, with values 0.5309 and 0.3906, respectively. The higher $\rho(r)$ value for the **TS1** suggests greater stability compared to the **TS2**, due to better distribution of charge along the transition state system. This is seen by comparing their $\Delta E^{\ddagger}$ and $\Delta G^{\ddagger}$ relative energies in Figures 3 and 4.

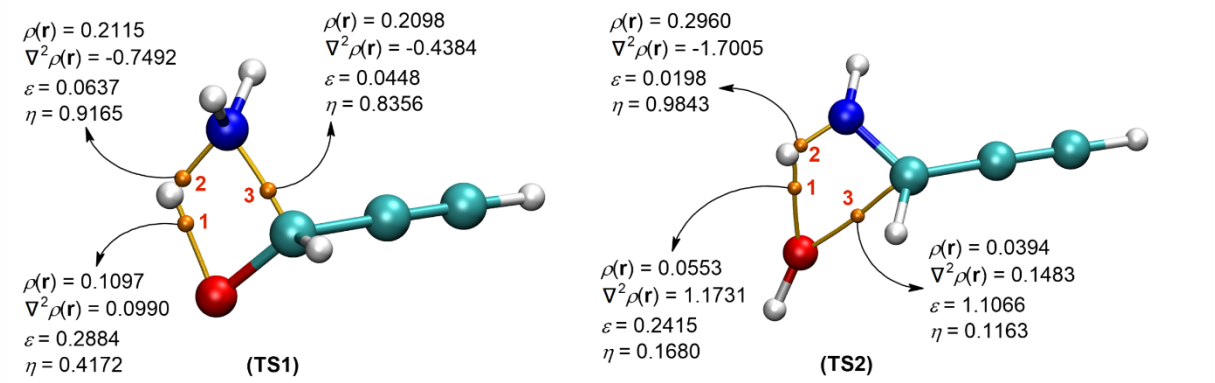

Fig 5. Molecular graphs of transition states (**TS1**, **TS2**) studied in the 10 K gas phase reaction model obtained from QTAIM analysis. Orange lines correspond to bond paths and orange spheres to bonds critical points along with electronic density, $\rho(r)$, Laplacian of the electron density, $\nabla^2\rho(r)$, Ellipticity of electron density, ε, and Electron localization function η. The bonds critical points analyzed are numbered in red.

Besides $\rho(r)$, we analyze other topological parameters of selected bond critical points using QTAIM[35–37] calculations as well as Laplacian of the electron density, $\nabla^2\rho(r)$ and Ellipticity of electron density, ε. According to the topological analysis of QTAIM, when $\rho(r)$ of the bond critical point is relatively high (x10^{-1} au) and $\nabla^2\rho(r) < 0$, the chemical interaction is defined as a shared shell and it is applied to covalent bond. In Figure 5 the values of $\rho(r)$ and $\nabla^2\rho(r)$ for critical points 2 and 3 (in red) in **TS1** indicate that H−N and N−C bond paths are shared shell interactions,[38] although the H-N bond critical point 2 is broken. On the other hand, the positive sign of Laplacian of the electron density ($\nabla^2\rho(r) > 0$) represents depletion of the electron density[39] as we can see in the Figure 5 for critical points 1 of **TS1**, even though the H-O is being formed. However, this value is similar to those from weak hydrogen bonds.[35,40,41] For **TS2** structure, the critical point 2 present relative high $\rho(r)$ value and $\nabla^2\rho(r) < 0$, while critical points 1 and 3 shows $\nabla^2\rho(r) > 0$ values. The ellipticity of electron density (ε) is defined in terms of the cylindricity of the $\rho(r)$ at the critical point constructed

from the eigenvalues of the Hessian matrix, λ_1 and λ_2 where $\varepsilon = |\lambda_1|/|\lambda_2| - 1$.[42] If $\lambda_1 = \lambda_2$ then $\varepsilon = 0$ and the bond is cylindrically symmetrical. Large ε values indicate structural instability. All critical points analyzed in the structures **TS1** show ε values, which are reasonably small indicating the stable character of binding. In the same way, the critical points 1 and 2 and 4 of **TS2** have low ε values. In contrast, in the critical point 3 of **TS2** structure the ε is in comparison reasonably high ($\varepsilon \approx 1.11$) which indicates that the $C \cdots O$ is an instable interaction.

The electron localization function (ELF), $\eta(r)$, is measured from the Fermi hole curvature in terms of the local excess kinetic energy density due to Pauli repulsion.43 When $\eta(r)$ values is confined to the [1,0] interval, the tendency to 1 means that parallel spins are highly improbable (otherwise opposite spin pairs are highly probable). On the other hand, the tendency to zero indicates a high probability of same spin pairs. As we can see in Figure 5 for critical points 2 and 3 of **TS1** show $\eta(r)$ values close to 1, indicating the presence of shared-shell interactions. Conversely, the critical point 1 have low $\eta(r)$ values indicate that bond paths are closed-shell interactions. Already **TS2** structures, critical point 2 show $\eta(r) \approx 1$ and critical points 1 and 3 show $\eta(r) \approx 0$.

Thus, critical points 1 and 2, following $\nabla^2\rho(r)$ and $\eta(r)$ values, show strong repulsion and attraction between H-O and H-N bond paths, being the reaction coordinate which increases energy barriers. Therefore, critical point 1 better summarizes the two reaction steps: in the **TS1** showing the formation of the N-C bond, and in **TS2** showing the elimination of the water molecule.

According to the PGIM formation mechanism model studied, the resulting product of the reaction (PGIM) is thermodynamically more stable than $\mathbf{R1}^{\mathbf{NH_3}}_{\mathbf{Prop}}$ with relative energies of $\Delta E = -1.67$ and $\Delta G = -0.98$ kcal $\cdot$ mol^{-1} for gas phase (Figure 3) while for the condensed phase the relative energies were $\Delta E = -1.97$ and $\Delta G = -0.02$ kcal $\cdot$ mol^{-1} (Figure 4). In other words, PGIM is energetically stable for both the 10 and 298 K gas phase reaction models. However, there is an stability increase when considering the 10 K ΔG, although the **TS1**, **TS2** energy barriers for the 10 K ISM model are lower than the 298 K model (Table 1).

In order to monitoring the interaction between the propynal and ammonia, we examined sp^n hybridization state of nitrogen atom in the reactant complexes, intermediate, transition states and product. The calculated sp^n hybridization state is summarized in Figure

6. Before the nucleophilic attack of the ammonia N atom, the hybridization is $sp^{3.33}$, with an almost perfect trigonal pyramidal shape. Then, after the nucleophilic attack, the hybridization decreases to $sp^{2.78}$ in **TS1**. Notably, at the N atom nucleophilic attack, **TS1** has a trigonal planar arrangement with an average angle that increases after the attack to more close the ideal 120°.[23] With the formation of **2**, the geometry becomes trigonal pyramidal again with hybridization $sp^{2.96}$. Finally, after release of the leaving group (H2O) and formation of **3**, its ends with an approximate trigonal pyramidal arrangement ($sp^{2.67}$) undergoing a decrease in the transition state **TS2** with hybridization $sp^{2.52}$.

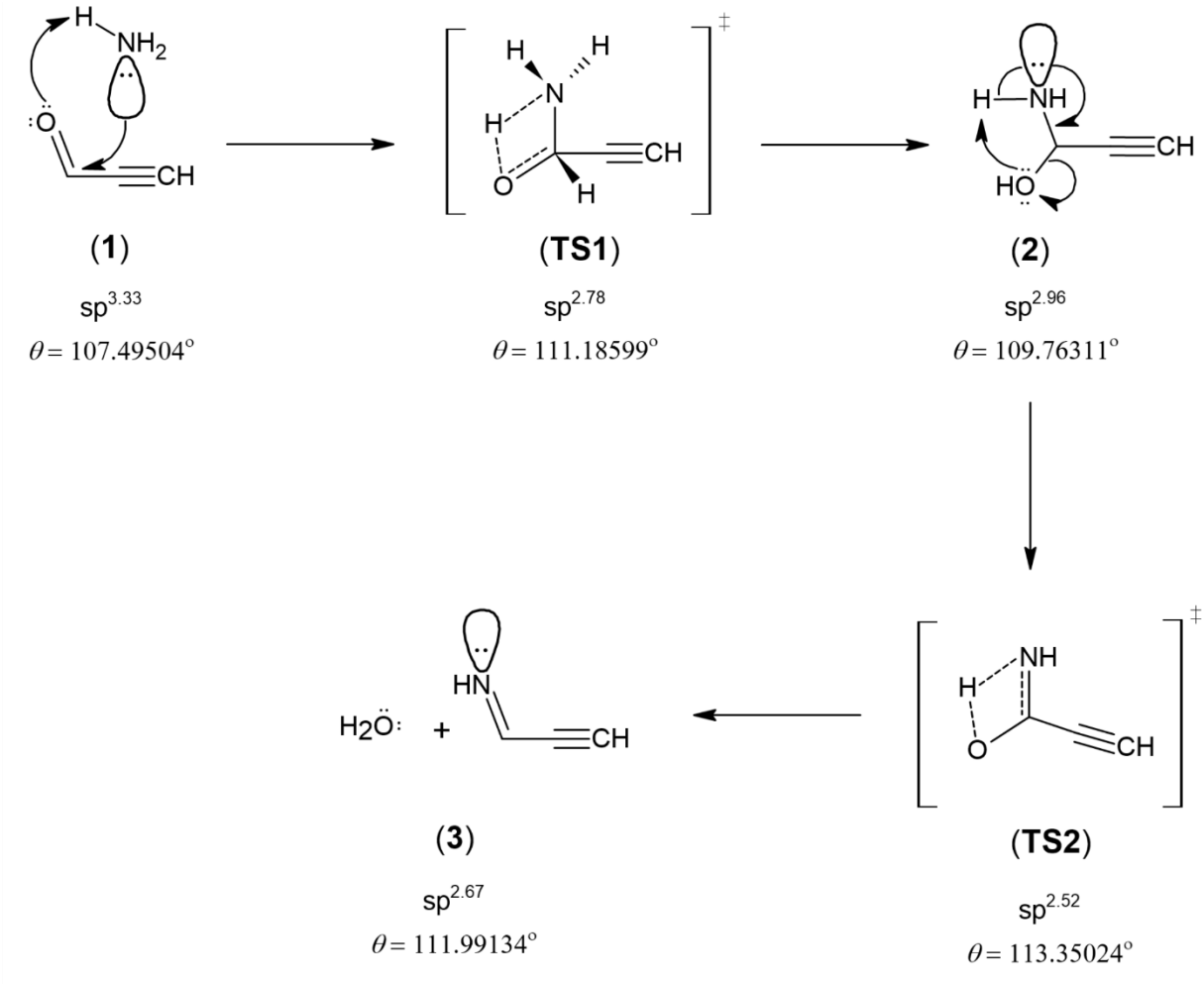

Fig 6. The hybridization analyses of the of the PGIM formation reaction. The pictorial representation shows the mean angle (θ) and hybridization index (n) of nitrogen atom for the reagents, transition states and PGIM final product.

3.4 Conclusion

The present study explored the mechanism of the PGIM synthesis through propynal and ammonia in ISM. We studied the mechanism for the reaction between propynal and ammonia in gas phase in 10 and 298 K by calculating the intermediate (**2**), transition state structures (**TS1** and **TS2**), and free-energy profiles for all of the elementary steps of the reaction, which takes place in two steps: (i) formation of a aminoalcohol by condensation of propynal with ammonia; and (ii) dehydration with the formation of 2-propyn-1-imine (PGIM) as the final product. The first step of the proposed reaction mechanism involves an S_N2 reaction with formation of intermediate **2** passing through a single biomolecular reaction step. The energy barrier for the first step, with 10 K, was $\Delta G^{\ddagger} = 33.73\ \text{kcal} \cdot \text{mol}^{-1}$. Whereas for the 298 K model reaction, the energy barrier has been increased to 41.54 $\text{kcal} \cdot \text{mol}^{-1}$. According to our results, the second step of the investigated mechanism suggests an E2 reaction with release of H_2O from **2**. The energy barrier of the second step of the 10 and 298 K gas-phase were $\Delta G^{\ddagger} = 46.66$ and 58.21 $\text{kcal} \cdot \text{mol}^{-1}$, respectively, showing also an increase in energy barrier. This study also showed that the PGIM final product is thermodynamically more stable than **1** for both the 10 and 298 K gas-phase model reactions. All the results of relative energies mentioned above, corroborate with the topological analyses and the other topological data obtained, particularly ε. The significant change in hybridization at the initial N_{ammonia} atom of $sp^{3.33}$ for an S_N2 reaction in the first step, modifies the electronic arrangement influencing the E2 reaction in the second step.

In a more general perspective, the results of our state-of-the-art computations provide convincing evidences about the feasibility of a general addition/elimination mechanism by Strecker synthesis for the formation of PGIM in ISM.

Data and Software Availability

QTAIM data was obtained with Multiwfn 3.8 (http://sobereva.com/multiwfn/). Images and visuals were made with ACD ChemSketch (https://www.acdlabs.com/) and Visual Molecular Dynamics (http://www.ks.uiuc.edu/Research/vmd/), both with an academic license. All electronic calculations were executed with Gaussian 09 Revision A.02 package (https://gaussian.com/) provided with UFC-CENAPAD (Centro Nacional de Processamento de

Alto Desempenho) computers. All other data obtained and analyzed during this study are provided or available for request upon reasonable solicitation.

Funding

This study was financed by the Brazilian agency Conselho Nacional de Desenvolvimento Científico e Tecnologico (CNPq). Lucas Coutinho thanks CAPES for his master's scholarship.

Declaration of Competing Interest

The authors report no conflicts of interest.

Acknowledgement

The authors also thank Centro Nacional de Processamento de Alto Desempenho (CENAPAD) of the Universidade Federal do Ceará (UFC) for providing computational resources.

Notes and references

(1) Herbst, E.; Van Dishoeck, E. F. Complex organic interstellar molecules. Annual Review of Astronomy and Astrophysics **2009**, 47, 427 – 480.

(2) Öberg, K. I.; Murray-Clay, R.; Bergin, E. A. The effects of snowlines on C/O in planetary atmospheres. The Astrophysical Journal Letters **2011**, 743, L16.

(3) McGuire, B. Census of Interstellar, Circumstellar, Extragalactic, Protoplanetary Disk, and Exoplanetary Molecules. arXiv **2021**. arXiv preprint arXiv:2109.13848 2021,

(4) Bizzocchi, L.; Prudenzano, D.; Rivilla, V. M.; Pietropolli-Charmet, A.; Giuliano, B. M.; Caselli, P.; Martín-Pintado, J.; Jiménez-Serra, I.; Martín, S.; Requena-Torres, M. A., *et al*. Propargylimine in the laboratory and in space: millimetre-wave spectroscopy and its first detection in the ISM. Astronomy & Astrophysics **2020**, 640, A98.

(5) Germain, A.; Tinacci, L.; Pantaleone, S.; Ceccarelli, C.; Ugliengo, P. Computer Generated

Realistic Interstellar Icy Grain Models: Physicochemical Properties and Interaction with NH3. ACS Earth and Space Chemistry **2022**, 6, 1286–1298.

(6) Herbst, E.; Klemperer, W. The formation and depletion of molecules in dense interstellar clouds. The Astrophysical Journal **1973**, 185, 505–534.

(7) Vidali, G.; Roser, J. E.; Ling, L.; Congiu, E.; Manicó, G.; Pirronello, V. The formation of interstellar molecules via reactions on dust grain surfaces. Faraday discussions **2006**, 133, 125–135.

(8) Singh, A.; Misra, A.; Tandon, P., *et al*. Quantum chemical analysis for the formation of glycine in the interstellar medium. Research in Astronomy and Astrophysics **2013**, 13, 912.

(9) Altwegg, K.; Balsiger, H.; Bar-Nun, A.; Berthelier, J.-J.; Bieler, A.; Bochsler, P.; Briois, C.; Calmonte, U.; Combi, M. R.; Cottin, H., *et al*. Prebiotic chemicals—amino acid and phosphorus—in the coma of comet 67P/Churyumov-Gerasimenko. Science advances **2016**, 2, e1600285.

(10) Woon, D. E. Pathways to glycine and other amino acids in ultraviolet-irradiated astrophysical ices determined via quantum chemical modeling. The Astrophysical Journal **2002**, 571, L177.

(11) Koch, D. M.; Toubin, C.; Peslherbe, G. H.; Hynes, J. T. A theoretical study of the formation of the aminoacetonitrile precursor of glycine on icy grain mantles in the interstellar medium. The Journal of Physical Chemistry C **2008**, 112, 2972–2980.

(12) Aponte, J. C.; Elsila, J. E.; Glavin, D. P.; Milam, S. N.; Charnley, S. B.; Dworkin, J. P. Pathways to meteoritic glycine and methylamine. ACS Earth and Space Chemistry **2017**, 1, 3–13.

(13) McDowell, S. A.; Arthurs, V. C. A computational study of binary gas-phase complexes of propargylimine, a recently detected molecule in the interstellar medium, with the molecules HF and H2O. Chemical Physics Letters **2022**, 790, 139296.

(14) Da Silva, J. G.; Santos, N.; Bonfils, X.; Delfosse, X.; Forveille, T.; Udry, S. Long-term magnetic activity of a sample of M-dwarf stars from the HARPS program-I. Comparison of activity indices. Astronomy & Astrophysics **2011**, 534, A30.

(15) Danger, G.; Borget, F.; Chomat, M.; Duvernay, F.; Theulé, P.; Guillemin, J.-C.; d'Hendecourt, L. L. S.; Chiavassa, T. Experimental investigation of aminoacetonitrile

formation through the Strecker synthesis in astrophysical-like conditions: reactivity of methanimine (CH2NH), ammonia (NH3), and hydrogen cyanide (HCN). Astronomy & Astrophysics **2011**, 535, A47.

(16) Strecker, A. Ueber die künstliche Bildung der Milchsäure und einen neuen, dem Glycocoll homologen Körper. Justus Liebigs Annalen der Chemie **1850**, 75, 27–45.

(17) Gardner, F.; Winnewisser, G. The detection of interstellar vinyl cyanide/acrylonitrile. The Astrophysical Journal **1975**, 195, L127–L130.

(18) Lupi, J.; Puzzarini, C.; Barone, V. Methanimine as a key precursor of imines in the interstellar medium: the case of propargylimine. The Astrophysical Journal Letters **2020**, 903, L35.

(19) de la Concepción, J. G.; Jiménez-Serra, I.; Corchado, J. C.; Rivilla, V. M.; Martín- Pintado, J. The origin of the E/Z isomer ratio of imines in the interstellar medium. The Astrophysical Journal Letters **2021**, 912, L6.

(20) Balucani, N.; Skouteris, D.; Ceccarelli, C.; Codella, C.; Falcinelli, S.; Rosi, M. A theoretical investigation of the reaction between the amidogen, NH, and the ethyl, C2H5, radicals: A possible gas-phase formation route of interstellar and planetary ethanimine. Molecular Astrophysics **2018**, 13, 30–37.

(21) Skouteris, D.; Balucani, N.; Ceccarelli, C.; Faginas Lago, N.; Codella, C.; Falcinelli, S.; Rosi, M. Interstellar dimethyl ether gas-phase formation: a quantum chemistry and kinetics study. Monthly Notices of the Royal Astronomical Society **2019**, 482, 3567–3575.

(22) Bader, R. F. A quantum theory of molecular structure and its applications. Chemical Reviews **1991**, 91, 893–928.

(23) Anslyn, E. V.; Dougherty, D. A. Modern physical organic chemistry; University science books, **2006**.

(24) Frisch, M.; Trucks, G. W.; Schlegel, H. B.; Scuseria, G. E.; Robb, M. A.; Cheeseman, J. R.; Scalmani, G.; Barone, V.; Mennucci, B.; Petersson, G., *et al*. Gaussian 09, revision D. 01. **2009**.

(25) Chai, J.-D.; Head-Gordon, M. Long-range corrected hybrid density functionals with damped atom–atom dispersion corrections. Phys. Chem. Chem. Phys. **2008**, 10, 6615–6620.

(26) Dunning, T. H. Gaussian basis sets for use in correlated molecular calculations. I. The

atoms boron through neon and hydrogen. The Journal of Chemical Physics **1989**, 90, 1007–1023.

(27) Gonzalez, C.; Schlegel, H. B. An improved algorithm for reaction path following. The Journal of Chemical Physics **1989**, 90, 2154–2161.

(28) Gonzalez, C.; Schlegel, H. B. Reaction path following in mass-weighted internal coordinates. Journal of Physical Chemistry **1990**, 94, 5523–5527.

(29) Bader, R. F. The quantum mechanical basis of conceptual chemistry. Monatshefte für Chemie/Chemical Monthly **2005**, 136, 819–854.

(30) Bader, R. F.; Nguyen-Dang, T. Advances in Quantum Chemistry; Elsevier, **1981**; Vol. 14; pp 63–124.

(31) Lu, T.; Chen, F. Multiwfn: a multifunctional wavefunction analyzer. Journal of computational chemistry **2012**, 33, 580–592.

(32) Rimola, A.; Sodupe, M.; Ugliengo, P. Deep-space glycine formation via Strecker-type reactions activated by ice water dust mantles. A computational approach. Physical Chemistry Chemical Physics **2010**, 12, 5285–5294.

(33) Puzzarini, C. Gas-phase Chemistry in the Interstellar Medium: The Role of Laboratory Astrochemistry. RNA World Hypothesis and the Origin of Life: Astrochemistry Perspective **2022**.

(34) Shingledecker, C. N.; Molpeceres, G.; Rivilla, V. M.; Majumdar, L.; Kästner, J. Isomers in interstellar environments. I. The case of Z-and E-cyanomethanimine. The Astrophysical Journal **2020**, 897, 158.

(35) Monteiro, N. K.; de Oliveira, J. F.; Firme, C. L. Stability and electronic structures of substituted tetrahedranes, silicon and germanium parents–a DFT, ADMP, QTAIM and GVB study. New Journal of Chemistry **2014**, 38, 5892–5904.

(36) Monteiro, N. K.; Firme, C. L. Hydrogen–hydrogen bonds in highly branched alkanes and in alkane complexes: a DFT, ab initio, QTAIM, and ELF study. The Journal of Physical Chemistry A **2014**, 118, 1730–1740.

(37) Bader, R. F. A bond path: a universal indicator of bonded interactions. The Journal of Physical Chemistry A **1998**, 102, 7314–7323.

(38) Kumar, P. S. V.; Raghavendra, V.; Subramanian, V. Bader's theory of atoms in molecules

(AIM) and its applications to chemical bonding. Journal of Chemical Sciences **2016**, 128, 1527–1536.

(39) Grabowski, S. J. Covalent character of hydrogen bonds enhanced by π-electron delocalization. Croatica Chemica Acta **2009**, 82, 185–192.

(40) Bone, R. G.; Bader, R. F. Identifying and analyzing intermolecular bonding interactions in van der Waals molecules. The Journal of Physical Chemistry **1996**, 100, 10892–10911.

(41) Boyd, R. J.; Choi, S. C. Hydrogen bonding between nitriles and hydrogen halides and the topological properties of molecular charge distributions. Chemical physics letters **1986**, 129, 62–65.

(42) Huang, W. J.; Momen, R.; Azizi, A.; Xu, T.; Kirk, S. R.; Filatov, M.; Jenkins, S. Nextgeneration quantum theory of atoms in molecules for the ground and excited states of fulvene. International Journal of Quantum Chemistry **2018**, 118, e25768.

(43) Becke, A. D.; Edgecombe, K. E. A simple measure of electron localization in atomic and molecular systems. The Journal of chemical physics **1990**, 92, 5397–5403.

4 CONCLUSION

In this work, the presented essays contribute to giving insights about the proposed mechanisms involving the psychedelic *N*,*N*-dimethyltryptamine and the interstellar medium (ISM) molecule propargylimine using computational chemistry methods.

In Chapter I, the double-methylation reaction route of tryptamine to biosynthesize DMT was explored with DFT calculations with the ONIOM QM:MM B3LYP/6-31+G(d,p):MM/UFF level of theory in order to describe the influence of the energy barriers involved in the reaction coordinate of both methylations. Based on the calculated energetic data, the PES profile of both methylations resembles S_N2 reactions, with the energy barriers of the first and second methylations being $\Delta G^{\ddagger} = 19.46$ and $33.80\ \text{kcal} \cdot \text{mol}^{-1}$, respectively. The MT energy barrier is $\delta G^{\ddagger} = 14.34\ \text{kcal} \cdot \text{mol}^{-1}$ larger than the tryptamine energy barrier, a behavior explained by the methyl group presence in the MT reagent impeding the second methyl donation. Besides, the change in hybridization at the initial MT reagent ($sp^{2.40}$) modifies the electronic arrangement influencing the second methylation acceptance of a methyl group. This also agrees with the NCI data indicating the first transition state to have less repulsive and more mild non-covalent interactions, and also the preference of the INMT enzyme for primary amines such as tryptamine, which are stronger nucleophiles than secondary amines. Thus, the energetic data shows that the double-methylation mechanism of DMT is an S_N2-like reaction, with the second methylation having the more considerable energy barrier and being the rate-limiting step. In addition, the second methylation higher energy barrier could be hypothesized as the one the reasons of low DMT human brain concentration, therefore, being significant to overcome this rate-limiting barrier to increase the DMT amount.

In Chapter II, the Strecker-type synthesis of the iCOM PGIM in the ISM was performed with the wB97XD/aug-cc-pVTZ level of theory to describe the mechanism of the propynal and ammonia reaction. The mechanism model was done in the gas phase in 10 and 298 K, in order to evaluate the ISM environment influence over the reactions, by DFT calculations of the intermediate (**2**), transition state structures (**TS1** and **TS2**), and free-energy profiles for the two-step reaction: the formation of a aminoalcohol by condensation of propynal with ammonia via a concerted S_N2 mechanism; and dehydration with the formation of 2-propyn-1-imine (PGIM) as the final product via an E2 water elimination mechanism. The energy barrier for the first step, with 10 K, was $\Delta G^{\ddagger} = 33.73\ \text{kcal} \cdot \text{mol}^{-1}$. Whereas for the 298 K model reaction, the energy barrier has been increased to 41.54 $\text{kcal} \cdot \text{mol}^{-1}$. The energy

barrier of the second step of the 10 and 298 K gas-phase were $\Delta G^{\ddagger} = 46.66$ and 58.21 kcal · mol^{-1}, respectively, showing also an increase in energy barrier, thus being the rate-limiting step. The obtained energy barriers demonstrate the ISM environment influence by favouring the reaction in lower temperature. Besides, the PGIM final product is thermodynamically more stable than **1** for both the 10 and 298 K gas-phase model reactions. The significant change in hybridization at the initial N_{ammonia} atom of $sp^{3.33}$ for an concerted S_N2 reaction in the first step, modifies the electronic arrangement influencing the E2 reaction in the second step. The topological analyses of QTAIM results correlate the energy barriers, particularly ρ and ε. Thus, the gathered data evidence that the obtained state-of-the-art calculations provide convincing evidences about the feasibility of a general mechanism by Strecker synthesis for the formation of PGIM in ISM.

Therefore, by gathering the theoretical results obtained, it is possible to verify the capacity of computational chemistry to analyze different chemical reactions, ranging from S_N2 to E2 mechanisms, and earthly-like enzyme systems to starlighted ones.

REFERENCES

ADAN, A. Chronotype and personality factors in the daily consumption of alcohol and psychostimulants. **Addiction**, v. 89, p. 455–462, 1994.

ALTWEGG, K.; BALSIGER, H.; BAR-NUN, A.; BERTHELIER, J.-J.; BIELER, A.; BOCHSLER, P.; BRIOIS, C.; CALMONTE, U.; COMBI, M. R.; COTTIN, H.; DE KEYSER, J.; DHOOGHE, F.; FIETHE, B.; FUSELIER, S. A.; GASC, S.; GOMBOSI, T. I.; HANSEN, K. C.; HAESSIG, M.; JÄCKEL, A.; KOPP, E.; KORTH, A.; LE ROY, L.; MALL, U.; MARTY, B.; MOUSIS, O.; OWEN, T.; RÈME, H.; RUBIN, M.; SÈMON, T.; TZOU, C.; WAITE, J. H.; WURZ, P. Prebiotic chemicals—amino acid and phosphorus—in the coma of comet 67P/Churyumov-Gerasimenko. **Science advances**, v. 2, p. e1600285, 2016.

ANSLYN, E.; DOUGHERTY, D. **Modern Physical Organic Chemistry**. 1. ed. [*S. l.*]: University Science Books, 2006.

APONTE, J. C.; ELSILA, J. E.; GLAVIN, D. P.; MILAM, S. N.; CHARNLEY, S. B.; DWORKIN, J. P. Pathways to meteoritic glycine and methylamine. **ACS Earth and Space Chemistry**, v. 1, p. 3–13, 2017.

BADER, R. F. A quantum theory of molecular structure and its applications. **Chemical Reviews**, v. 91, p. 893–928, 1991.

BARKER, S. A. *N*,*N*-dimethyltryptamine (DMT), an endogenous hallucinogen: Past, present, and future research to determine its role and function. **Frontiers in Neuroscience**, v. 12, 2018.

BIZZOCCHI, L.; PRUDENZANO, D.; RIVILLA, V. M.; PIETROPOLLI-CHARMET, A.; GIULIANO, B. M.; CASELLI, P.; MARTÍN-PINTADO, J.; JIMÉNEZ-SERRA, I.; MARTÍN, S.; REQUENA-TORRES, M. A.; RICO-VILLAS, F.; ZENG, S.; GUILLEMIN, J. C. Propargylimine in the laboratory and in space: millimetre-wave spectroscopy and its first detection in the ISM. **Astronomy & Astrophysics**, v. 640, n. A98, 2020.

CHUNG, L. W.; HIRAO, H.; LI, X.; MOROKUMA, K. The oniom method: its foundation and applications to metalloenzymes and photobiology. **WIREs Computational Molecular Science**, v. 2, n. 2, p. 327–350, 2012.

DANGER, G.; BORGET, F.; CHOMAT, M.; DUVERNAY, F.; THEULÉ, P.; GUILLEMIN, J.-C.; D'HENDECOURT, L. L. S.; CHIAVASSA, T. Experimental investigation of aminoacetonitrile formation through the Strecker synthesis in astrophysical-like conditions: reactivity of methanimine (CH_2NH), ammonia (NH_3), and hydrogen cyanide (HCN). **Astronomy & Astrophysics**, v. 535, n. A47, 2011.

DE LA CONCEPCIÓN, J. G.; JIMÉNEZ-SERRA, I.; CORCHADO, J. C.; RIVILLA, V. M.; MARTÍN- PINTADO, J. The origin of the E/Z isomer ratio of imines in the interstellar medium. **The Astrophysical Journal Letters**, v. 912, n. L6, 2021.

FONTECAVE, M.; ATTA, M.; MULLIEZ, E. *S*-adenosylmethionine: nothing goes to waste. **Trends in Biochemical Sciences**, v. 29, n. 5, p. 243–249, 2004. ISSN 0968-0004.

FRISCH, M. J.; TRUCKS, G. W.; SCHLEGEL, H. B.; SCUSERIA, G. E.; ROBB, M. A.; CHEESEMAN, J. R.; SCALMANI, G.; BARONE, V.; MENNUCCI, B.; PETERSSON, G. A.; NAKATSUJI, H.; CARICATO, M.; LI, X.; HRATCHIAN, H. P.; IZMAYLOV, A. F.; BLOINO, J.; ZHENG, G.; SONNENBERG, J. L.; HADA, M.; EHARA, M.; TOYOTA, K.; FUKUDA, R.; HASEGAWA, J.; ISHIDA, M.; NAKAJIMA, T.; HONDA, Y.; KITAO, O.; NAKAI, H.; VREVEN, T.; MONTGOMERY Jr., J. A.; PERALTA, J. E.; OGLIARO, F.; BEARPARK, M.; HEYD, J. J.; BROTHERS, E.; KUDIN, K. N.; STAROVEROV, V. N.; KOBAYASHI, R.; NORMAND, J.; RAGHAVACHARI, K.; RENDELL, A.; BURANT, J. C.; IYENGAR, S. S.; TOMASI, J.; COSSI, M.; REGA, N.; MILLAM, J. M.; KLENE, M.; KNOX, J. E.; CROSS, J. B.; BAKKEN, V.; ADAMO, C.; JARAMILLO, J.; GOMPERTS, R.; STRATMANN, R. E.; YAZYEV, O.; AUSTIN, A. J.; CAMMI, R.; POMELLI, C.; OCHTERSKI, J. W.; MARTIN, R. L.; MOROKUMA, K.; ZAKRZEWSKI, V. G.; VOTH, G. A.; SALVADOR, P.; DANNENBERG, J. J.; DAPPRICH, S.; DANIELS, A. D.; FARKAS, ; FORESMAN, J. B.; ORTIZ, J. V.; CIOSLOWSKI, J.; FOX, D. J. **Gaussian 09 Revision A.02**. Wallingford, CT: Gaussian, Inc., 2009. Gaussian, Inc., Wallingford, CT, USA.

GALLIMORE, A. R.; STRASSMAN, R. J. A model for the application of target controlled intravenous infusion for a prolonged immersive DMT psychedelic experience. **Frontiers in Pharmacology**, v. 7, 2016. ISSN 1663-9812.

GLYNOS, N. G.; CARTER, L.; LEE, S. J.; KIM, Y.; KENNEDY, R. T.; MASHOUR, G. A.; WANG, M. M.; BORJIGIN, J. Indolethylamine *N*-methyltransferase (INMT) is not essential for endogenous tryptamine-dependent methylation activity in rats. **Scientific Reports**, v. 13, n. 280, 2023.

GUERRA-DOCE, E. Psychoactive Substances in Prehistoric Times: Examining the Archaeological Evidence. **Time and Mind**, v. 8, p. 91–112, 2015.

JAMIESON, C. S.; MISA, J.; TANG, Y.; BILLINGSLEY, J. M. Biosynthesis and synthetic biology of psychoactive natural products. **Chemical Society Reviews journal**, v. 50, p. 6950–7008, 2021.

LUPI, J.; PUZZARINI, C.; BARONE, V. Methanimine as a key precursor of imines in the interstellar medium: the case of propargylimine. **The Astrophysical Journal Letters**, v. 903, n. 2, 2020.

MANSKE, R. H. F. A synthesis of the methyltryptamines and some derivatives. **Canadian Journal of Research**, v. 5, n. 5, p. 592–600, 1931.

MCDOWELL, S. A.; ARTHURS, V. C. A computational study of binary gas-phase complexes of propargylimine, a recently detected molecule in the interstellar medium, with the molecules HF and H_2O. **Chemical Physics Letters**, v. 790, p. 139296, 2022.

MCKENNA, T. **Food of the Gods: The Search for the Original Tree of Knowledge a Radical History of Plants, Drugs, and Human Evolution**. 1. ed.; Bantam New Age Books: New York, 1993.

NICHOLS, D. *N*,*N* -dimethyltryptamine and the pineal gland: Separating fact from myth. **Journal of Psychopharmacology**, v. 32, p. 026988111773691, 2017.

RIMOLA, A.; SODUPE, M.; UGLIENGO, P. Deep-space glycine formation via Strecker-type reactions activated by ice water dust mantles. A computational approach. **Physical Chemistry Chemical Physics**, v. 12, p. 5285–5294, 2010.

SAMORINI, G. The oldest archeological data evidencing the relationship of Homo sapiens with psychoactive plants: A worldwide overview. **Journal of Psychedelic Studies**, v. 3, p. 1–18, 2019.

SANDFORD, S. A.; NUEVO, M.; BERA, P. P.; LEE, T. J. Prebiotic astrochemistry and formation of molecules of astrobiological interest in interstellar clouds and protostellar disks. **Chemical Reviews**, v. 120, p. 616-4659, 2020.

SEPARATA DE ARQUIVOS DO I.P.A. Observações sobre "Vinho da Jurema" Utilizado pelos índios Pancarú de Tacaratú (Pernambuco). Recife, Brazil, 1946.

STRASSMAN, R. J.; QUALLS, C. R. Dose-Response Study of N,N-Dimethyltryptamine in Humans: I. Neuroendocrine, Autonomic, and Cardiovascular Effects. **Archives of General Psychiatry**, v. 51, n. 2, p. 85–97, 1994. ISSN 0003-990X.

STRASSMAN, R. J.; QUALLS, C. R.; UHLENHUTH, E. H.; KELLNER, R. Dose-Response Study of *N,N*-Dimethyltryptamine in Humans: II. Subjective Effects and Preliminary Results of a New Rating Scale. **Archives of General Psychiatry**, v. 51, n. 2, p. 98–108, 02 1994. ISSN 0003-990X.

SZÁRA, S. Dimethyltryptamin: Its metabolism in man; the relation of its psychotic effect to the serotonin metabolism. **Experientia**, v. 12, n. 11, p. 441–442, 1956.

ZHANG, J.; ZHENG, Y. G. SAM/SAH analogs as versatile tools for SAM-dependent methyltransferases. **ACS Chemical Biology**, v. 11, n. 3, p. 583–597, 2016. PMID: 26540123.

APPEENDIX A - AUTOR´S CURRICULAR DATA

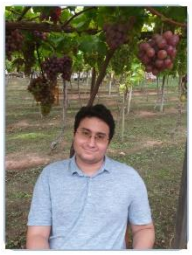

Lucas Pinheiro Coutinho

Bolsista de Mestrado do CNPq

Endereço para acessar este CV: http://lattes.cnpq.br/5120273208842910
ID Lattes: **5120273208842910**
Última atualização do currículo em 20/04/2023

Pesquisador, em conclusão de mestrado em química (foco em físico-química), em Universidade Federal do Ceará (UFC). Formado em química bacharelado (2017-2021) em UFC. Atualmente é bolsista CNPq de mestrado no Grupo de Química Téorica (GQT). Tem experiência em Química Teórica e Computacional. Anteriormente, estudou Catálise Heterogênea na conversão de glicerol por catalisadores metálicos no Laboratório de Adsorção e Catálise (LANGMUIR) e simulações de dinâmica molecular (DM) de sistemas biológicos e modelos mecânico-quânticos para avaliação de atividades biológicas empregando Teoria Funcional da Densidade (DFT) no GQT, na qualidade de iniciação científica em UFC. Atualmente, estuda a elucidação do mecanismo de reação através de cálculos teóricos híbridos ONIOM/QM:MM na elucidação de mecanismos de reações biológicas em humanos, métodos quânticos como QTAIM e Fukui para análise de corantes e simulações DM para desenvolvimento de novos materiais. **(Texto informado pelo autor)**

Identificação

Nome	Lucas Pinheiro Coutinho
Nome em citações bibliográficas	COUTINHO, L. P.;COUTINHO, LUCAS P.;COUTINHO, LUCAS PINHEIRO
Lattes iD	http://lattes.cnpq.br/5120273208842910

Endereço

Formação acadêmica/titulação

2022	Mestrado em andamento em QUÍMICA. Universidade Federal do Ceará, UFC, Brasil. Orientador: Norberto de Kássio Vieira Monteiro. Coorientador: Sérgio Ruschi Bergamachi Silva. Bolsista do(a): Conselho Nacional de Desenvolvimento Científico e Tecnológico, CNPq, Brasil.
2017 - 2021	Graduação em Química. Universidade Federal do Ceará, UFC, Brasil. Título: Proposta de um modelo mecânico-quântico para avaliar a atividade antioxidante de compostos fenólicos dos extratos aquosos de Curcuma longa L., Piper nigrum L. e Cuminum cyminum empregando teoria funcional da densidade. Orientador: Norberto de Kássio Vieira Monteiro.
2014 - 2016	Ensino Médio (2º grau). Organização Farias Brito, FB, Brasil.

Formação Complementar

2019 - 2019	Modelagem Computacional. (Carga horária: 6h). Universidade Federal do Ceará, UFC, Brasil.
2017 - 2017	Análise Térmica. (Carga horária: 4h). Universidade Federal do Ceará, UFC, Brasil.
2013 - 2015	PBF Advanced Course. (Carga horária: 226h). PBF, PBF, Brasil.

Atuação Profissional

Universidade Federal do Ceará, UFC, Brasil.

Vínculo institucional

2017 - Atual Vínculo: , Enquadramento Funcional:

Projetos de pesquisa

2022 - Atual

Estudo teórico do mecanismo de formação do alucinógeno N,N-dimetiltriptamina (DMT)
Descrição: Algumas substâncias psicodélicas, como a dimetiltriptamina (DMT), são agonistas serotonérgicos potentes com capacidade de modular funções cerebrais como memória e cognição. Essa classe de substâncias têm apresentado potencial terapêutico para diversos transtornos mentais e dependência química. No entanto, o fato de ser produzida endogenamente em mamíferos torna a DMT particularmente interessante. Sua biossíntese faz parte da cascata bioquímica do triptofano e ocorre após a dupla metilação da triptamina pela enzima INMT. Os detalhes moleculares dessas reações são quase inexistentes. Logo, propõe-se um estudo computacional, utilizando química quântica, para elucidar o mecanismo reacional enzimático de produção de DMT endógeno, bem como quantificar as barreiras de ativação envolvidas. A descrição molecular da rota enzimática poderá também dar suporte para um processo biotecnológico verde de produção exógena em larga escala..
Situação: Em andamento; Natureza: Pesquisa.
Alunos envolvidos: Mestrado acadêmico: (1) .

Integrantes: Lucas Pinheiro Coutinho - Integrante / MONTEIRO, NORBERTO DE KÁSSIO VIEIRA - Coordenador / Sérgio Ruschi Bergamachi Silva - Integrante.

2018 - 2020

Simulação de Dinâmica Molecular das interações entre Fármacos e Membranas Biológicas
Descrição: Projeto PIBIC/UFC (2018 - 2020) A obesidade é uma doença crônica não transmissível (DCNT) decorrente, principalmente, do excesso de gordura no tecido adiposo visceral, que dificulta vários processos metabólicos, ocasionando problemas de caráter multifatorial. Os tratamentos contemporâneos para a obesidade envolvem intervenção dietoterápica acompanhada de atividade física adequada e do uso de fármacos como sibutramina, orlistate e Saxenda®. Apesar disso, o uso de medicamentos pode causar efeitos colaterais, existindo a necessidade de desenvolvimento de novos fármacos. Nesta vertente, trabalhos na literatura afirmam que inibidores de tripsina de diferentes origens podem contribuir no tratamento da obesidade e prevenção de doenças consequentes, através do estímulo à secreção de colecistocinina (CCK) e leptina, hormônios relacionados com a saciedade. Desse modo, o sequenciamento do inibidor de tripsina de tamarindo purificado (ITTp) da semente de tamarindo (Tamarindus indica L.) deixou lacunas resultando em uma sequência primária incompleta, dificultando a caracterização do ITTp. Sendo assim, estudos computacionais podem fornecer um entendimento sobre esses sistemas através de simulações de dinâmica molecular (DM). Utilizando o algoritmo Blastp e o repositório de arquivos RCSB, foram feitos o alinhamento inicial, que substituiu as lacunas do ITTp pelos resíduos de aminoácidos da sequência com maior identidade percentual, e o alinhamento múltiplo, que escolheu as quatro sequências com as maiores identidades percentuais. As sequências escolhidas foram utilizadas para criação, através do software MODELLER 9.21, de 150 modelos homólogos, selecionando-se 5 deles pela pontuação DOPE (do inglês Discrete Optimized Protein Energy), e apurando o modelo mais realista no programa MOLPROBITY a partir de determinados critérios. O modelo apurado foi submetido a uma DM no programa GROMACS 2018.4 para estabilização e comprovação de que ele era suportado pelo software. Após a validação do modelo tridimensional criado, o programa CONCOORD 2.1.2 foi utilizado para gerar 500 conformações do ITTp, selecionando 4 conformações estáveis utilizando o critério de soma de violações. Após isso, estas conformações passaram por uma DM, calculando-se o RMSD (do inglês Root-Mean-Square Deviation) e a Energia de Interação total (EIT), selecionando a conformação com 3 a maior tempo de interação e com a menor Energia de Interação total (EIT), -301.012837 Kcal.mol -1 . Por fim, a Energia de Interação por Resíduo (EIR) foi calculada, identificando os resíduos de aminoácidos ARG 59, ARG 63, ILE 54, PRO 57 e GLU 78 como os participantes do ITTp na interação. Dentre os resíduos, as duas argininas tiveram maior contribuição, evidenciando que a interação ITTp-tripsina se dá principalmente através de interações coulombianas, com o principal sítio ativo do ITTp interagindo com a superfície de carga parcial negativa da tripsina..
Situação: Concluído; Natureza: Pesquisa.

Integrantes: Lucas Pinheiro Coutinho - Integrante / Norberto de Kássio Vieira Monteiro - Coordenador.

2017 - 2018

Síntese de acetol via processo catalítico para valorização do glicerol
Descrição: Projeto PIBIC - PIBIC 2017/2018 - Edital 03/17 O aumento da produção de biodiesel e a falta de mercado para oglicerol acabou provocando decréscimo do seu valor

comercial. Devido asua estrutura química, três grupos ?OH em uma curta cadeia carbônica (C3H8O3), o glicerol é uma substância relativamente versátil a qual estápropícia a vária reações. Podendo ser destacadas as reações dedesidratação, hidrogenólise e de oxidação. Esses processos propiciam aobtenção de produtos de elevado valor comercial, tais como: acetol eacroleína (desidratação), 1,2- e 1,3-propanodiol (hidrogenólise), ácido glicérico, ácido lático, ácido oxálico (oxidação), dentre outros. O presente projeto tem como objetivo gerar produtos de maior valor agregado a partirdo glicerol utilizando catalise heterogênea. A proposta visa sintetizar diferentes materiais contendo óxido de cobre disperso em suporte ácidocomo o óxido de molibdênio e antimônio. Objetiva-se conduzir o processo em fase gasosa e em fase líquida. Industrialmente a fase líquida é maisviável, no entanto, o estudo reacional em fase gasosa auxilia na elucidação do processo catalítico. O processo de valorização do glicerol é uma pesquisa relevante para a cadeia do biodiesel, haja visto que a relação entre o custo de produção e o valor de mercado do biodiesel, pode prejudicar sua sustentabilidade econômica..
Situação: Concluído; Natureza: Pesquisa.

Integrantes: Lucas Pinheiro Coutinho - Coordenador / Antoninho Valentini - Integrante.

Áreas de atuação

1. Grande área: Ciências Exatas e da Terra / Área: Química / Subárea: Química.
2. Grande área: Ciências Exatas e da Terra / Área: Química / Subárea: Química Teórica.

Idiomas

Inglês Compreende Razoavelmente, Fala Bem, Lê Razoavelmente, Escreve Razoavelmente.

Produções

Produção bibliográfica

Artigos completos publicados em periódicos

Ordenar por

Ordem Cronológica

1. FREITAS, M. A. ; MACHADO, RAYNARA I. A ; ROCHA, ISABELLE H. M. ; LIMA, LORENA S ; **COUTINHO, LUCAS PINHEIRO** ; MONTEIRO, NORBERTO DE KÁSSIO VIEIRA ; L. NETO, PEDRO ; MAZZETTO, SELMA E. ; ROCHA, HUGO A. O. ; MACHADO, RICHELE J. A . Determination of phenolic compounds and antioxidant potential of aqueous extracts of Curcuma longa L., Piper nigrum L. and Cuminum cyminum: an experimental and a quantum-mechanical study. JOURNAL OF HEALTH & BIOLOGICAL SCIENCES, v. 10, p. 1-10, 2022.

2. DE MEDEIROS, AMANDA FERNANDES ; DE SOUZA, BEATRIZ BLENDA PINHEIRO ; **COUTINHO, LUCAS PINHEIRO** ; MURAD, ALINE MELRO ; DOS SANTOS, PAULA IVANI MEDEIROS ; MONTEIRO, NORBERTO DE KÁSSIO VIEIRA ; SANTOS, ELIZEU ANTUNES DOS ; MACIEL, BRUNA LEAL LIMA ; DE ARAÚJO MORAIS, ANA HELONEIDA . Structural insights and molecular dynamics into the inhibitory mechanism of a Kunitz-type trypsin inhibitor from Tamarindus indica L. JOURNAL OF ENZYME INHIBITION AND MEDICINAL CHEMISTRY JCR, v. 36, p. 480-490, 2021.

Citações: WEB OF SCIENCE℠ 6

3. COSTA, JOSÉ DE RIBAMAR M. ; SANTOS, REGINA C.R. ; **COUTINHO, LUCAS P.** ; SILVA, ODERLANDO R. ; BARROS, HELENILSON O. ; FREIRE, VALDER N. ; VALENTINI, ANTONINHO . CO2 role on the glycerol conversion over catalyst containing CaO-SiO2 doped with Ag and Pt. CATALYSIS TODAY JCR, v. 1, p. 1, 2019.

Citações: WEB OF SCIENCE℠ 4

Textos em jornais de notícias/revistas

1. **COUTINHO, L. P.**; JUNIOR, M. . Efeitos do Óxido de Antimônio nas Propriedades Ácidas do Óxido de Alumínio. Revista Encontros Universitários, p. 1173 - 1173.
2. **COUTINHO, L. P.**; MONTEIRO, N. K. V. . Estudo de Simulações Computacionais de Dinâmica Molecular de Sistemas Biológicos Envolvidos com a Diabete Mellitus Tipo 2. Revista Encontros Universitários, p. 1437 - 1437.
3. **COUTINHO, L. P.**; MONTEIRO, N. K. V. . DETERMINAÇÃO DE COMPOSTOS FENÓLICOS E POTENCIAL ANTIOXIDANTE DE EXTRATOS AQUOSOS DE CURCUMA LONGA L., PIPER NIGRUM L. E CUMINUM CYMINUM: UM ESTUDO DE MECÂNICA QUÂNTICA. Revista Encontros Universitários, p. 1033 - 1033.
4. **COUTINHO, L. P.**; SANTOS, REGINA C.R. ; VALENTINI, A. . Síntese de Acetol Via Processo Catalítico para Valorização do Glicerol. Revista Encontros Universitários, p. 1917 - 1917.

Resumos publicados em anais de congressos

1. **COUTINHO, L. P.**; SANTOS, R. C. R. ; VALENTINI, A. . SÍNTESE DE ACETOL VIA PROCESSO CATALÍTICO PARA VALORIZAÇÃO DO GLICEROL. In: XXXVII Encontro de Iniciação Científica - Encontros Universitários, 2018, Fortaleza. XXXVII Encontro de Iniciação Científica - Encontros Universitários, 2018.
2. VALERO, J. M. ; SILVA, O. R. ; **COUTINHO, L. P.** ; VALENTINI, A. . EFEITO DO DIÓXIDO DE CARBONO SOBRE A CONVERSÃO DE GLICEROL EMPREGANDO CATALISADORES CONTENDO CAO DOPADO COM PRATA OU PLATINA. In: XXXVII Encontro de Iniciação Científica - Encontros Universitários, 2018, Fortaleza. XXXVII Encontro de Iniciação Científica - Encontros Universitários, 2018.
3. **COUTINHO, L. P.**; JUNIOR, M. ; VALENTINI, A. . EFEITOS DO ÓXIDO DE ANTIMÔNIO NAS PROPRIEDADES ÁCIDAS DO ÓXIDO DE ALUMÍNIO. In: XXXVI Encontro de Iniciação Científica - Encontros Universitários, 2017, Fortaleza. XXXVI Encontro de Iniciação Científica - Encontros Universitários, 2018.

Apresentações de Trabalho

1. **COUTINHO, L. P.**. Do MCVM à Pesquisa Científica. 2022. (Apresentação de Trabalho/Comunicação).
2. **COUTINHO, LUCAS PINHEIRO**; MONTEIRO, NORBERTO DE KÁSSIO VIEIRA . PROPOSTA DE UM MODELO MECÂNICO-QUÂNTICO PARA AVALIAR A ATIVIDADE ANTIOXIDANTE DOS EXTRATOS AQUOSOS DE Curcuma longa L., Piper nigrum L. E Cuminum cyminum EMPREGANDO TEORIA FUNCIONAL DA DENSIDADE. 2022. (Apresentação de Trabalho/Outra).
3. **COUTINHO, L. P.**; MONTEIRO, N. K. V. . Determinação de Compostos Fenólicos e Potencial Antioxidante de Extratos Aquosos de Curcuma Longa L., Piper Nigrum L. E Cuminum Cyminum: um Estudo de Mecânica Quântica. 2020. (Apresentação de Trabalho/Outra).
4. **COUTINHO, L. P.**; MONTEIRO, N. K. V. . Estudo de Simulações Computacionais de Dinâmica Molecular de Sistemas Biológicos Envolvidos com a Diabete Mellitus Tipo 2. 2019. (Apresentação de Trabalho/Outra).
5. **COUTINHO, L. P.**; SANTOS, REGINA C.R. ; VALENTINI, A. . Síntese de Acetol Via Processo Catalítico para Valorização do Glicerol. 2018. (Apresentação de Trabalho/Outra).
6. **COUTINHO, L. P.**; JUNIOR, M. . Efeitos do Óxido de Antimônio nas Propriedades Ácidas do Óxido de Alumínio. 2017. (Apresentação de Trabalho/Outra).

Eventos

Participação em eventos, congressos, exposições e feiras

1. XI SEMANA DA QUÍMICA E IV WORKSHOP DA PÓS-GRADUAÇÃO EM QUÍMICA. 2020. (Outra).
2. XXXIX Encontro de Iniciação Científica.Determinação de Compostos Fenólicos e Potencial Antioxidante de Extratos Aquosos de Curcuma Longa L., Piper Nigrum L. E Cuminum Cyminum: um Estudo de Mecânica Quântica. 2020. (Encontro).
3. X Semana da Química da UFC e III Workshop da Pós-Graduação em Química. 2019. (Outra).
4. XXXVIII Encontro de Iniciação Científica.Estudo de Simulações Computacionais de Dinâmica Molecular de Sistemas Biológicos Envolvidos com a Diabete Mellitus Tipo 2. 2019. (Encontro).
5. XXXVI Encontro de Iniciação Científica - Universidade Federal do Ceará.TOS DO ÓXIDO DE ANTIMÔNIO NAS PROPRIEDADESÁCIDAS DO ÓXIDO DE ALUMÍNIO. 2018. (Encontro).
6. XXXVII Encontro de Iniciação Científica - Encontros Universitários.SÍNTESE DE ACETOL VIA PROCESSO CATALÍTICO PARA VALORIZAÇÃO DO GLICEROL. 2018. (Outra).
7. III Semana Pré-Reação de Química. 2017. (Outra).
8. Encontros Universitários - Universidade Federal do Ceará - 2016. 2016. (Outra).

ANNEX A - PAPERS'S DRAFT PROOF AND PUBLISHED PAPERS

(SUBMITTED)

Organic & Biomolecular Chemistry

Organic & Biomolecular Chemistry

A mechanistic insight for the biosynthesis of N,N-dimethyltryptamine: an ONIOM theoretical approach

Journal:	*Organic & Biomolecular Chemistry*
Manuscript ID	Draft
Article Type:	Paper
Date Submitted by the Author:	n/a
Complete List of Authors:	Coutinho, Lucas; Universidade Federal do Ceara Centro de Ciencias, Departamento de Química Analítica e Físico-Química Silva, Sérgio; Universidade Federal do Rio Grande do Norte, Instituto de Química; Instituto do Cérebro Lima-Neto, Pedro; Universidade Federal do Ceará, Quimica Analitica e Físico-Quimica Monteiro, Norberto; Universidade Federal do Ceara,
Note: The following files were submitted by the author for peer review, but cannot be converted to PDF. You must view these files (e.g. movies) online.	
freq_Gibbs_Free_Energy_Correction.zip sp_Electronic_Energy.zip	

(SUBMITTED)

Planetary and Space Science

A computational study of the propargylimine (PGIM) formation mechanism in the interstellar medium (ISM).

--Manuscript Draft--

Manuscript Number:	PSS-D-23-00113
Article Type:	Research Paper
Keywords:	Interstellar medium; PGIM; DFT; mechanism; QTAIM; ELF

Corresponding Author:	Norberto Monteiro Federal University of Ceara BRAZIL
First Author:	Lucas Coutinho
Order of Authors:	Lucas Coutinho
	Norberto Monteiro

Abstract:	Theoretical quantum chemistry studies of reaction mechanisms involving molecules of the interstellar medium (ISM) are essential to understand the origin of organic matter in the space environment. Here, computational chemistry was used to investigate the Strecker synthesis leading to the formation of interstellar molecule propargylimine. Our proposal for a two-step mechanism of PGIM synthesis involved the WB97XD/aug-ccpVTZ level of theory in the gas phase at temperatures of 10K and 298K. Based on the energetic data, the Potential Energy Surface (PES) indicates an SN2 mechanism for the first step and an SN1 elimination mechanism for the second step, with a lower energy barrier considering the first step. The results suggest that the PGIM product is thermodynamically more stable than the reactants. Furthermore, topological data from QTAIM and ELF agree with the energetic data. Therefore, these results demonstrate that PGIM can be formed through two-step Strecker synthesis in a possible interstellar environment.

Suggested Reviewers:	CARLOS HUITLE carlos.alberto.mh@ufrn.br
	Pedro Neto pln@ufc.br
	Escamilla Roa roa@iaa.es
	Ryan C. Fortenberry r410@olemiss.edu
Opposed Reviewers:	Caio Firme caio.firme@ufrn.br I have personal problems with this researcher, this may influence the decision on the manuscript.

(SUBMITTED)

Degradation of xanthene-based dyes by photoactivated persulfate: experimental and computational studies

Carlos Pedro G. do Nascimento[a§], Mateus S. M. A. Costa[a§], Jessica M. A. Freire[b], Luiz Thiago V. da Silva[a], Lucas P. Coutinho[a], Norberto K. V. Monteiro[a*], Davila de S. Zampieri[c]; Juliene T. Oliveira[a], Ronaldo F. do Nascimento[a], Idalina M. M. de Carvalho[c], Helena Becker[a], Elisane Longhinotti[a*]

[a]*Departamento de Química Analítica e Físico-Química, Universidade Federal do Ceará, 60455-900, Fortaleza - CE, Brazil*

[b]*Seara da Ciência, Universidade Federal do Ceará, 60455-320, Fortaleza - CE, Brazil*

[c]*Departamento de Química Orgânica e Inorgânica, Universidade Federal do Ceará, 60455-900, Fortaleza - CE, Brazil*

[§]*Carlos Pedro G. do Nascimento and Mateus S. M. A. Costa contributed equally to this paper.*

Corresponding Author:

*Norberto K.V. Monteiro: norbertokv@ufc.br

(PUBLISHED)

J. Health Biol Sci. 2022;10(1):1-10 doi: 10.12662/2317-3206jhbs.v10i1.3859.p1-10.2022

ORIGINAL ARTICLE

Determination of phenolic compounds and antioxidant potential of aqueous extracts of *Curcuma longa* L., *Piper nigrum* L. and *Cuminum cyminum*: an experimental and a quantum-mechanical study

Determinação de compostos fenólicos e potencial antioxidante dos extratos aquosos de *Curcuma longa* L., *Piper nigrum* L. e *Cuminum cyminum*: um estudo experimental e quanto-mecânico.

Morgana A. Freitas[1], Raynara I. A. Machado[2], Isabelle H. M. Rocha[1], Lorena S. Lima[1], Lucas P. Coutinho[3], *Norberto K. V. Monteiro[4], Pedro de L. Neto[4], Selma E. Mazzetto[4], Hugo A. O. Rocha[5], Richele J. A. Machado[6]

1. Discente do curso de Nutrição no Centro Universitário Christus (UNICHRISTUS), Fortaleza, CE, Brasil. 2. Mestre pelo Departamento de Bioquímica, Universidade Federal do Rio Grande do Norte, Natal, RN, Brasil. 3. Graduação pelo Departamento de Química Analítica e Físico-Química, Universidade Federal do Ceará, Fortaleza, CE, Brasil. 4. Docente do Programa de Pós-graduação em química, Universidade Federal do Ceará (UFC), Fortaleza, CE, Brasil. 5. Docente do programa de Pós-graduação em bioquímica, Universidade Federal do Rio Grande do Norte (UFRN), Natal, RN, Brasil. 6. Docente do Curso de Graduação em Nutrição no Centro Universitário Christus (UNICHRISTUS), Fortaleza, CE, Brasil.

Abstract

Objectives: Evaluation of phenolic compounds and antioxidant activities of aqueous extracts of *C. longa*, *P. nigrum* and *C. cyminum*. In addition to proposing a quantum-mechanical model to evaluate the antioxidant activity. **Methods**: The aqueous extracts were prepared using roots of the *Curcuma longa* L., seeds of the *Piper nigrum L.* and seeds of *Cuminum cyminum*. The extracts were subjected to tests to detect and quantify phenolic compounds and to assess their antioxidant capacity by different methods. Furthermore, to investigate the electronic nature of the antioxidant activity of the main compounds present in these extracts, frontier molecular orbitals (FMOs) were obtained by the DFT/B3LYP/6-31G(d,p) level of theory. **Results**: After statistical analysis of the results, a greater number of phenolic compounds and better antioxidant activity was identified in the aqueous extracts of cumin (*C. cyminum*) in all three assays performed, when compared to the other extracts tested. The theoretical model based on the Pietro method is in agreement with the experimental results. **Conclusion**: This study has an innovative proposal with the trivial antioxidant activity combined with theoretical quantum-mechanical calculations that can serve to reduce costs and time and to predict the antioxidant activity of subsequent studies.

Keywords: Bioactive Compounds; Antioxidant Activities; Density Functional Theory; Frontier Molecular Orbitals.

Resumo

Objetivos: avaliar os compostos fenólicos e atividades antioxidantes dos extratos aquosos de *C. longa*, *P. nigrum* e *C. cyminum* bem como propor um modelo quanto-mecânico para avaliar a atividade antioxidante. **Métodos**: os extratos aquosos foram preparados por meio da utilização de raízes de *Curcuma longa* L., sementes de *Piper nigrum* L. e sementes de *Cuminum cyminum*. Os extratos foram submetidos a ensaios para detectar e quantificar compostos fenólicos e atividade antioxidante por diferentes métodos. Além disso, com objetivo de investigar a natureza eletrônica da atividade antioxidante dos principais compostos presentes nesses extratos, orbitais moleculares de fronteira (OMFs) foram obtidos pelo nível de teoria DFT/B3LYP/6-31G(d,p). **Resultados**: após as análises estatísticas dos resultados, a maior quantidade de compostos fenólicos com maior atividade antioxidante foi identificada no extrato aquoso do cominho (*C. cyminum*) em todos os ensaios realizados, quando comparados com os outros extratos testados. O modelo teórico baseado no método de Pietro está concordante com os resultados experimentais. **Conclusão**: este estudo possui uma proposta inovadora com a atividade antioxidante trivial combinada com cálculos quanto-mecânicos que podem servir para reduzir custos e tempo para predizer a atividade antioxidante de estudos futuros.

Palavras-chave: Compostos Bioativos. Atividades Antioxidante. Teoria Funcional da Densidade. Orbitais Moleculares de Fronteira.

INTRODUCTION

Oxidative stress is often associated with pathological conditions such as cancer, neurodegenerative disorders, cardiovascular disease, diabetes mellitus, acute and chronic kidney disease (CKD)[1,2]. The antioxidant plays a central role in the termination of oxidative chain reactions by removing the free radical intermediates[3]. Polyphenols are secondary metabolites from plants with antioxidant potential used in the prevention of diseases related to oxidative stress[4]. Many studies have been conducted to identify new natural antioxidants[2].

Plants and their constituents have been used in the treatment of diseases since antiquity. The use of medicinal plants is an economical and accessible way to treat the population, contributing to primary health care[5]. These constituents are

Correspondence: Norberto de Kássio Vieira Monteiro. Departamento de Química Analítica e Físico-Química. Universidade Federal do Ceará - Campus do Pici. CEP 60020-181. E-mail: norbertokv@ufc.br
Conflict of interest: The authors declare that there is no conflict of interest.
Received: 2021 Apr 13; Revised: 2021 Oct 20; Accepted: 2021 Nov 26

(PUBLISHED)

Journal Pre-proof

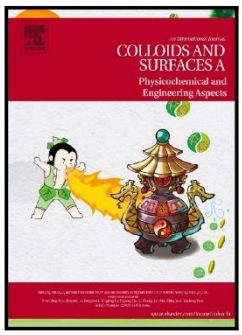

Analysis of Fe^{2+} and Mn^{2+} ions in DES and water: A theoretical study using Molecular Dynamic Simulations, QTAIM and NCI-RDG

Laudenor Amorim, Renato Veríssimo de Oliveira, Lucas Lima Bezerra, Lucas Pinheiro Coutinho, Pierre Basílio Almeida Fechine, Adriana Nunes Correia, Ámison Rick Lopes da Silva, Pedro de Lima-Neto, Norberto Kássio de Vieira Monteiro

PII: S0927-7757(23)00902-0

DOI: https://doi.org/10.1016/j.colsurfa.2023.131818

Reference: COLSUA131818

To appear in: *Colloids and Surfaces A: Physicochemical and Engineering Aspects*

Received date: 14 April 2023
Revised date: 29 May 2023
Accepted date: 4 June 2023

Please cite this article as: Laudenor Amorim, Renato Veríssimo de Oliveira, Lucas Lima Bezerra, Lucas Pinheiro Coutinho, Pierre Basílio Almeida Fechine, Adriana Nunes Correia, Ámison Rick Lopes da Silva, Pedro de Lima-Neto and Norberto Kássio de Vieira Monteiro, Analysis of Fe^{2+} and Mn^{2+} ions in DES and water: A theoretical study using Molecular Dynamic Simulations, QTAIM and NCI-RDG, *Colloids and Surfaces A: Physicochemical and Engineering Aspects,* (2023) doi:https://doi.org/10.1016/j.colsurfa.2023.131818